

CONDITIONAL PARTICLE FILTERS WITH BRIDGE BACKWARD SAMPLING

SANTERI KARPPINEN, SUMEETPAL S. SINGH, MATTI VIHOLA

ABSTRACT. The performance of the conditional particle filter (CPF) with backward sampling is often impressive even with long data records. However, when the observations are weakly informative relative to the dynamic model, standard multinomial resampling is wasteful and backward sampling has limited effect. In particular, with time-discretised continuous-time path integral models, backward sampling degenerates in refined discretisations. We detail two conditional resampling strategies suitable for the weakly informative regime: the so-called ‘killing’ resampling and the systematic resampling with mean partial order. To avoid the degeneracy issue of backward sampling, we introduce a generalisation that involves backward sampling with an auxiliary ‘bridging’ CPF step, which is parameterised by a blocking sequence. We present practical tuning strategies for choosing an appropriate blocking. Our experiments demonstrate that the CPF with a suitable resampling and the developed ‘bridge backward sampling’ can lead to substantial efficiency gains in the weakly informative regime.

1. INTRODUCTION

Conditional particle filter (CPF) with multinomial resampling and backward sampling (BS) [1, 33] can perform well with challenging state-space models and long data records [23]. However, when the observations are weakly informative, the commonly used multinomial resampling introduces excess noise, and when the dynamic model is slow mixing, backward sampling has only a limited effect. The aim of this paper is to consider CPFs in such ‘weak potential’ scenarios, which arise for instance with time-discretisations of Feynman–Kac (FK) path integral models.

Arnaudon and Del Moral [3] considered a continuous-time version of the CPF in the case of killing resampling, and derived convergence rate results for it, which are analogous with the convergence rates obtained for the discrete-time CPF [2, 26]. Motivated by successes of CPF with BS (hereafter CPF-BS) in the discrete time domain, we were interested to seek for a BS analogue which is stable with respect to refined time-discretisations. It is relatively easy to see that the direct application of BS degenerates under such refined discretisations, except for limited cases such as when the driving Markov process admits jumps, such as considered in [27], or in a univariate case where the trajectories can cross with positive probability.

The main contributions of this paper are as follows.

- We detail two new conditional resampling algorithms: the ‘killing’ and systematic resampling with mean partition (Section 5). These are conditional versions of resampling algorithms, which are stable in the weak potentials setting (in the continuous-time limit) [6]. We also detail a generic sufficient condition for conditional resamplings (Assumption 7), which guarantees validity of the CPF (Theorem 2), and complements the result of [5].
- We introduce a new CPF with bridge backward sampling (CPF-BBS) (Section 6), which may be regarded as a generalisation of BS to an arbitrary ‘blocking sequence,’ and which can avoid the degeneracy problem of CPF-BS with refined discretisations.

- The performance of the CPF-BBS relies on an appropriately chosen blocking sequence, which depends on the model at hand. Therefore, a significant portion of our work focuses on finding practical, computationally inexpensive and robust tuning criteria for choosing such a sequence (Section 7). The method requires a small number of independent runs of the standard particle filter for the model of interest.

The CPF-BBS is a general method, but requires evaluation of and simulation from the conditional distributions of (multiple steps of the) proposal distributions. In practice, this typically means that the proposals are linear-Gaussian, arising for instance from a linear stochastic differential equation (SDE).

The CPF-BBS features ‘bridging’ CPF steps, which resemble the intermediate block importance sampling suggested in [25], and the MCMC rejuvenation considered in [4, 25]; there are similarities also with the bridging particle filter suggested in [12]; see also [28]. We believe that our approach is more efficient than direct importance bridging, and because our approach can be intuitively related to a continuous-time analogue (through [6]), it is expected to behave well with respect to refinement of time-discretisation, unlike the MCMC bridging.

Our experiments (Section 9) demonstrate how the developed resamplings outperform standard multinomial resampling in the weak potential setting, and we establish empirically an order between their performance, which follows a similar pattern as the results of [6] for the standard particle filter applied to FK path integral models. Empirical results using the CPF-BBS show a significant improvement over CPF-BS in the weak potential setting, and reveal how the method is stable with respect to refined discretisation. Finally, our tuning algorithm appears to deliver blocking sequences that reach near-optimal performance with little additional specification from the user.

2. PRELIMINARIES AND NOTATION

We aim at inference of a probability density on \mathbf{X}^T with the following form:

$$(1) \quad \pi(x_{1:T}) = \frac{\eta(x_{1:T})}{\mathcal{Z}}, \quad \text{where} \quad \eta(x_{1:T}) := M_1(x_1)G_1(x_1) \prod_{k=2}^T M_k(x_k \mid x_{k-1})G_k(x_{k-1:k}).$$

The model above, defined in terms of $M_{1:T}$ and $G_{1:T}$, is often referred to as a Feynman-Kac (FK) model [10]. Here, $M_1(x_1)$ and $M_k(x_k \mid x_{k-1})$ define, respectively, an initial distribution and ‘proposal’ transition densities of a Markov chain on \mathbf{X} , and $G_1 : \mathbf{X} \rightarrow [0, \infty)$ and $G_k : \mathbf{X}^2 \rightarrow [0, \infty)$ for $k \geq 2$ are called ‘potential’ or ‘weight’ functions (see the discussion below). The probability π is well-defined assuming that the normalising constant $\mathcal{Z} := \int \eta(x_{1:T})dx_{1:T} \in (0, \infty)$.

Above, and hereafter, ‘ dx ’ stands for a σ -finite dominating measure on \mathbf{X} , integers are equipped with the counting measure, and product spaces are equipped with products of the dominating measures. We use the shorthand notation of the form $x_{a:b} = (x_a, \dots, x_b)$ and $x_{a:b}^{i_a:i_b} = (x_a^{i_a}, \dots, x_b^{i_b})$. We also denote $[N] := \{1, \dots, N\}$. Test and potential functions are implicitly assumed measurable.

The FK model can be seen as a slight generalisation of the hidden Markov model (HMM), which has a latent Markov state $X_{1:T}$ with initial (prior) density $m_1(x_1)$ and transition probability densities $m_k(x_k \mid x_{k-1})$, and conditional independent observations $y_{1:T}^*$ with observation densities $g_k(y_k \mid x_k)$. The posterior (or smoothing) distribution of $X_{1:T} \mid y_{1:T}^*$ is of form (1) if we choose $M_k \equiv m_k$ and $G_k(\cdot) \equiv g_k(y_k^* \mid \cdot)$. However, it is often beneficial to choose another ‘proposal’ family $M_k \not\equiv m_k$, in which case the ‘weights’ are

$G_1(x_1) := g_1(y_k^* \mid x_1)m_1(x_1)/M_1(x_1)$ and $G_k(x_k) := g_k(y_k^* \mid x_k)m_k(x_k \mid x_{k-1})/M_k(x_k \mid x_{k-1})$ for $k \geq 2$.

3. THE PARTICLE FILTER

The particle filter is a sequential Monte Carlo algorithm, which includes sampling from Markov dynamics M_k , and *resampling* proportional to weights arising from G_k . The resampling operation $r(a^{1:N} \mid g^{1:N})$ defines a probability distribution on $[N]^N$ which depends on non-negative ‘unnormalised weights’ $g^{1:N}$. That is, if $A^{1:N} \sim r(\cdot \mid g^{1:N})$ in $[N]$, then $\mathbb{P}(A^{1:N} = a^{1:N}) = r(a^{1:N} \mid g^{1:N})$. We will only consider *unbiased resamplings* [7] r , which means that for all $j \in [N]$:

$$(2) \quad \left(\sum_{i=1}^N g^i \right) \mathbb{E}_{r(\cdot \mid g^{1:N})} \left[\frac{1}{N} \sum_{i=1}^N \mathbf{1}(A^i = j) \right] = g^j.$$

Algorithm 1 describes the particle filter targetting the FK model (1) using N particles, and an unbiased resampling r . The boldface notation $\mathbf{X}_1^{(i)} = X_1^{(i)}$ and $\mathbf{X}_{k+1}^{(i)} = (X_k^{(A_k^{(i)})}, X_{k+1}^{(i)})$ stands for the latest particles augmented with their ancestors, generated during the algorithm. In what follows, we use underline to denote ‘all particles’ at one time

Algorithm 1 PF($r, M_{1:T}, G_{1:T}, N$)

- 1: Draw $X_1^{(i)} \sim M_1(\cdot)$ for $i \in [N]$.
- 2: Set $\mathbf{X}_1^{(i)} = X_1^{(i)}$ for $i \in [N]$.
- 3: **for** $k = 1, \dots, T-1$ **do**
- 4: Set $W_k^{(i)} = G_k(\mathbf{X}_k^{(i)})$ for $i \in [N]$.
- 5: Draw $A_k^{(1:N)} \sim r(\cdot \mid W_k^{(1:N)})$
- 6: Draw $X_{k+1}^{(i)} \sim M_{k+1}(\cdot \mid X_k^{(A_k^{(i)})})$ for $i \in [N]$.
- 7: Set $\mathbf{X}_{k+1}^{(i)} = (X_k^{(A_k^{(i)})}, X_{k+1}^{(i)})$ for $i \in [N]$.
- 8: **end for**
- 9: Set $W_T^{(i)} = G_T(\mathbf{X}_T^{(i)})$ for $i \in [N]$.
- 10: **output** $(X_{1:T}^{(1:N)}, A_{1:T-1}^{(1:N)}, W_{1:T}^{(1:N)})$

instant, so for instance $\underline{X}_k = X_k^{(1:N)}$.

Consider then the following density on $\mathbf{X}^{NT} \times [N]^{N(T-1)}$ which corresponds to the variables generated during Algorithm 1:

$$(3) \quad \zeta^{(N)}(\underline{x}_{1:T}, \underline{a}_{1:T-1}) = \prod_{i=1}^N M_1(x_1^{(i)}) \prod_{k=1}^{T-1} \left(r(\underline{a}_k \mid G_k(\underline{x}_k)) \prod_{i=1}^N M_{k+1}(x_{k+1}^{(i)} \mid x_k^{a_k^{(i)}}) \right).$$

The normalising constant estimate calculated from $\underline{X}_{1:T}$ and $\underline{A}_{1:T-1}$ in the output of Algorithm 1, is defined as follows:

$$(4) \quad \hat{\mathcal{Z}}(\underline{x}_{1:T}, \underline{a}_{1:T-1}) = \prod_{k=1}^T \left(\frac{1}{N} \sum_{i=1}^N G_k(\mathbf{x}_k^i) \right).$$

Thanks to the unbiasedness of the resampling (2), the following ‘unbiasedness property’ [cf. 10] holds, which is key for the validity of particle Markov chain Monte Carlo algorithms [1]:

$$(5) \quad \mathbb{E}[\hat{\mathcal{Z}}(\underline{X}_{1:T}, \underline{A}_{1:T-1}) f(X_{1:T}^*)] = \mathcal{Z} \mathbb{E}_\pi[f(X_{1:T})].$$

Equation (5) holds for any test function $f : X^T \rightarrow \mathbb{R}$ for which the expectation on the right is well-defined, as long as the trajectory $X_{1:T}^* = X_{1:T}^{(B_{1:T})}$ is chosen among all particles in a suitable manner, that is, with suitably generated indices $B_{1:T}$.

The most direct approach is to draw $B_T \sim \text{Categ}(\omega_T^{(1:N)})$ with (unnormalised weights) $\omega_T^{(i)} = G_T(\mathbf{X}_T^{(i)})$, and to set the rest of the indices recursively by ‘ancestor tracing’: $B_k := A_k^{(B_{k+1})}$. In our case, where the potentials depend on at most two consecutive states, it is possible to replace ancestor tracing by ‘backward sampling’: for $k = T-1, \dots, 1$:

$$B_k \sim \text{Categ}(\omega_k^{(1:N)}) \quad \text{where} \quad \omega_k^{(i)} := G_k(\mathbf{X}_k^{(i)}) G_{k+1}(X_k^{(i)}, X_{k+1}^{(B_{k+1})}) M_{k+1}(X_{k+1}^{(B_{k+1})} \mid X_k^{(i)}).$$

The unbiasedness (5) was shown in [9] for ancestor tracing and multinomial resampling, and has been extended for other unbiased resamplings [e.g. 1]. For the context of the present work, we refer the reader to [31, Appendix D] for a proof of the unbiasedness assuming only unbiasedness of resampling (2), and which accommodates backward sampling with any resampling.

4. THE CONDITIONAL PARTICLE FILTER

The CPF introduced in [1] implements a π -invariant Markov update from a ‘reference’ path $X_{1:T}^* \in X^T$ to a newly chosen path $\tilde{X}_{1:T}^* \in X^T$. The original scheme of [1] assumed multinomial sampling with ancestor tracing, and [33] suggested, in a discussion note to [1], that backward sampling may also be used (with multinomial resampling); later an algorithmic variant of BS called ‘ancestor sampling’ (AS) [24] was also introduced. In fact, the corresponding Markov kernels are reversible with respect to π , and BS/AS is guaranteed to outperform AT in the asymptotic variance sense [5]. The improvement has been found substantial in many empirical studies; see also [23] for a theoretical result supporting such findings.

Algorithm 2 presents a generic version of the CPF with N particles and with ancestor tracing, using a generic conditional resampling $r^{(p,n)}$. The conditional resampling scheme

Algorithm 2 CPF-AT($r^{(p,n)}$, $X_{1:T}^*$, $B_{1:T}$; $M_{1:T}$, $G_{1:T}$, N)

- 1: $(\underline{X}_{1:T}, \underline{A}_{1:T-1}, B_T) \leftarrow \text{CPF}(r^{(p,n)}, X_{1:T}^*, B_{1:T}; M_{1:T}, G_{1:T}, N)$
- 2: $\tilde{B}_{1:T-1} \leftarrow \text{ANCESTORTRACE}(\underline{A}_{1:T-1}, \tilde{B}_T)$.
- 3: **output** $(\tilde{X}_{1:T}^*, \tilde{B}_{1:T})$ where $\tilde{X}_{1:T}^* = X_{1:T}^{(\tilde{B}_{1:T})}$.

Algorithm 3 CPF($r^{(p,n)}$, $X_{1:T}^*$, $B_{1:T}$; $M_{1:T}$, $G_{1:T}$, N)

- 1: Draw $X_1^{(-B_1)} \sim M_1(\cdot)$ and set $X_1^{(B_1)} \leftarrow X_1^*$ and $\mathbf{X}_1^{(i)} = X_1^{(i)}$ for $i \in [N]$.
- 2: **for** $k = 1, \dots, T-1$ **do**
- 3: $A_k^{(1:N)} \leftarrow r^{(B_k, B_{k+1})}(\cdot \mid G_k(\mathbf{X}_k^{(1:N)}))$
- 4: Draw $X_{k+1}^{(i)} \sim M_{k+1}(\cdot \mid X_k^{(A_k^{(i)})})$ for $i \neq B_{k+1}$ and set $X_{k+1}^{(B_{k+1})} = X_{k+1}^*$.
- 5: Set $\mathbf{X}_{k+1}^{(i)} = (X_k^{(A_k^{(i)})}, X_{k+1}^{(i)})$ for $i \in [N]$.
- 6: **end for**
- 7: Draw $\tilde{B}_T \sim \text{Categ}(G_T(\mathbf{X}_T^{(1:N)}))$.
- 8: **output** $(\underline{X}_{1:T}, \underline{A}_{1:T-1}, \tilde{B}_T)$

draws the ancestor indices (on line 3 of Algorithm 3) conditional on the ancestor of the

Algorithm 4 ANCESTORTRACE($a_{\ell:u-1}, b_u$)

```

for  $v = u - 1, u - 2, \dots, \ell$  do  $b_v \leftarrow a_v^{(b_{v+1})}$ 
output  $b_{\ell:u-1}$ .

```

reference. This makes it possible to write Algorithm 2 such that the reference trajectory can be located at arbitrary indices $B_{1:T}$, unlike earlier formulations, which assume reference at index 1 [e.g. 5]. The arbitrary reference indices turn out to be convenient for us, when we introduce the bridge backward sampling CPF in Section 6. Definition 1 gives a sufficient condition that $r^{(p,n)}$ is a valid conditional resampling for use with Algorithm 2.

Definition 1. The conditional resampling scheme $r^{(p,n)}(\cdot \mid g^{(1:N)})$ is valid, if it is a conditional of an unconditional unbiased symmetric resampling scheme $r(\cdot \mid g^{(1:N)})$. That is, for all $g^{(1:N)} \geq 0$ such that $\sum_{\ell=1}^N g^{(\ell)} > 0$, and all $p, n \in \{1:N\}$,

- (i) $\mathbb{P}_{r^{(p,n)}(\cdot \mid g^{(1:N)})}(A^{(n)} = p) = 1$,
- (ii) $r^{(p,n)}(a^{(1:n)} \mid g^{(1:N)}) = \mathbb{P}_{r(\cdot \mid g^{(1:N)})}(A^{(-n)} = a^{(-n)} \mid A^{(n)} = p)$,
- (iii) $\mathbb{P}_{r(\cdot \mid g^{(1:N)})}(A^{(n)} = p) = \frac{g^{(p)}}{\sum_{i=1}^N g^{(i)}}$.

Theorem 2. Algorithm 2 with a valid conditional resampling $r^{(p,n)}$ defines a Markov update $(X_{1:T}^*, B_{1:T}) \rightarrow (\tilde{X}_{1:T}^*, \tilde{B}_{1:T})$ that is reversible with respect to $\pi \times U(\{1:N\}^T)$.

Theorem 2, whose proof is given in Appendix A, complements the result of [5] by accommodating our version of the CPF, where the reference is placed at arbitrary position, and allows for the resamplings which we discuss next.

5. CONDITIONAL RESAMPLINGS FOR THE WEAK POTENTIALS SCENARIO

The simplest unbiased resampling, that is, satisfying (2) is *multinomial resampling*, where A^k are drawn independently from the categorical distribution $\text{Categ}(w^{1:N})$ with normalised weights $w^j = \frac{g^j}{\sum_{i=1}^N g^i}$. However, in the context of this work, multinomial resampling is wasteful, and we focus instead on conditional versions of two resampling algorithms, that were found stable in refined discretisations [6].

The first of these is the ‘killing’ resampling, defined as follows [cf. 11]:

$$(6) \quad r_{\text{kill}}(a^{(1:N)} \mid g^{(1:N)}) := \prod_{i=1}^N \left[\mathbf{1}(a^{(i)} = i) \frac{g^{(i)}}{g^*} + \left(1 - \frac{g^{(i)}}{g^*}\right) \sum_{j=1}^N \mathbf{1}(a^{(i)} = j) \frac{g^{(j)}}{\sum_{\ell=1}^N g^{(\ell)}} \right],$$

where $g^* = \max_{i \in \{1:N\}} g^{(i)}$ (and in case $g^* = 0$, ρ may be defined arbitrarily). The killing resampling is valid also with any other choice of g^* as long as $g^{(j)} \leq g^*$, but we consider the above one minimising the resampling rate.

Killing resampling is simple and stable, but [6] found two resamplings that yield a smaller resampling rate, and appear to admit slightly better performance: the Srinivasan sampling process (SSP) and systematic resampling, both with mean partition order. It seems difficult to implement a conditional version of SSP (in an efficient manner), but systematic resampling with mean partition can be implemented by extending the algorithm of [5].

The systematic resampling with mean partition (Definition 5) is a variant of ‘standard’ systematic resampling (Definition 3) where the weights $w^{1:N}$ are processed in a particular ‘mean partition’ order (Definition 4). The mean partition may be found in $O(N)$ time, and our implementation is based on Hoare’s scheme [20]; see Algorithm 12 in Appendix E.

Definition 3. (Systematic resampling). Input normalised weights $w^{1:N}$. Simulate a single $\tilde{U} \sim U(0, 1)$, set $\check{U}^i := (i-1+\tilde{U})/N$ and define the resampling indices as $A^i := F^{-1}(\check{U}^i)$ for $i \in [N]$. Here, the generalised inverse $F^{-1}(u)$ is defined for $u \in (0, 1)$ as the unique index $i \in [N]$ such that $F(i-1) < u \leq F(i)$, with $F(i) := \sum_{j=1}^i w^j$.

Definition 4. (Mean partition order) Suppose that $u^{1:N} \in \mathbb{R}^N$. A permutation $\varpi : [N] \rightarrow [N]$ is a *mean partition* order for $u^{1:N}$, if the re-indexed vector $u_{\varpi}^i := u^{\varpi(i)}$ satisfies $u_{\varpi}^1, \dots, u_{\varpi}^m \leq \bar{u}$ and $u_{\varpi}^{m+1}, \dots, u_{\varpi}^N > \bar{u}$ for some $m \in [N]$, with \bar{u} denoting the mean of the vector u .

Definition 5. (Systematic resampling with mean partition). Let F_{ϖ}^{-1} denote the generalised inverse distribution function corresponding to the re-indexed weights $w_{\varpi}^{1:N}$, where ϖ is a mean partition order as in Definition 4. Set $A^{\varpi(i)} := \varpi(F_{\varpi}^{-1}(\check{U}^i))$, where $\check{U}^{1:N}$ are defined as in Definition 3.

Algorithms 5 and 6 describe the conditional variants of killing resampling and systematic resampling with mean partition, respectively.

Algorithm 5 Conditional killing resampling $\rho_{\text{kill}}^{(i,k)}(\cdot \mid g^{(1:N)})$.

- 1: Draw $\bar{A}^{(1:N)} \sim \rho_{\text{kill}}(\cdot \mid g^{(1:N)})$.
- 2: Draw $J \in \{1:N\}$ such that

$$\mathbb{P}(J = j) = h(j \mid i) := \begin{cases} \frac{1}{N} \left(1 + \frac{\sum_{\ell \neq i} g^{(\ell)}}{g^*} \right), & j = i \\ \frac{1}{N} \left(1 - \frac{g^{(j)}}{g^*} \right), & j \neq i. \end{cases}$$

- 3: Set $S := \llbracket J - k \rrbracket_N$, where $\llbracket \ell \rrbracket_N := 1 + (\ell - 1 \bmod N)$.
- 4: Set $\bar{A}^{(\llbracket k+S \rrbracket_N)} \leftarrow i$.
- 5: **output** $A^{(1:N)}$ where $A^{(j)} = \bar{A}^{(\llbracket j+S \rrbracket_N)}$

Algorithm 6 Conditional systematic resampling with mean partition $\rho_{\text{syst}}^{(i,k)}(\cdot \mid g^{(1:N)})$.

- 1: For $j \in [N]$, define $W^j := \frac{g^{(j)}}{\sum_{i=1}^N g^{(i)}}$ and $U^j := \frac{j-1+U}{N}$, where $U \sim U(0, 1)$.
- 2: Set $r = NW^i - \lfloor NW^i \rfloor$ and $p = \frac{r(\lfloor NW^i \rfloor + 1)}{NW^i}$.
- 3: With probability p , draw $\bar{U} \sim U(0, r)$ and set $N^i = \lfloor NW^i \rfloor + 1$; otherwise draw $\bar{U} \sim U(r, 1)$ and set $N^i = \lfloor NW^i \rfloor$.
- 4: Set $\varpi \leftarrow \text{MEANPARTITIONORDER}(W^{1:N})$ ▷ Algorithm 12 in Appendix E
- 5: Set $s = \varpi^{-1}(i)$ and $\tilde{\varpi} = \sigma_{1-s}(\varpi)$, so that $\tilde{\varpi}(1) = \varpi(s) = i$.
- 6: Draw $\bar{A}^{\tilde{\varpi}(1:N)} = \tilde{\varpi}(F_{\tilde{\varpi}}^{-1}(U^{[N]}))$.
- 7: Draw $C \sim U([N])$ and set $A^j = \bar{A}^{\sigma_{k-C}(j)}$, for $j \in [N]$.
- 8: **output** $A^{1:N}$.

Lemma 6. The following define valid conditional resamplings (Definition 1):

- (i) conditional killing $\rho_{\text{kill}}^{(i,k)}(\cdot \mid g^{(1:N)})$ of Algorithm 5, and
- (ii) conditional systematic resampling with mean partition $\rho_{\text{syst}}^{(i,k)}$ of Algorithm 6.

Proof of Lemma 6 is given in Appendix A.

6. THE CONDITIONAL PARTICLE FILTER WITH BRIDGE BACKWARD SAMPLING

The conditional particle filter with bridge backward sampling (CPF-BBS), which we consider next, requires tractable Markov dynamics $\{M_k\}$, that is:

Assumption 7. Denote $M_{\ell:u}(x_{\ell:u}) := \prod_{k=\ell+1}^u M_k(x_k | x_{k-1})$ for any $2 \leq \ell < u \leq T$. Then, we are able to simulate from and evaluate the density of the conditional distribution of x_ℓ given $x_{\ell-1}$ and x_u :

$$\bar{M}_\ell(x_\ell | x_{\ell-1}, x_u) := \frac{\int M_{\ell-1:u}(x_{\ell-1:u}) dx_{\ell+1:u-1}}{M_{u|\ell-1}(x_u | x_{\ell-1})}.$$

Furthermore, we assume that we are able to evaluate the conditional density of x_u given x_ℓ :

$$M_{u|\ell}(x_u | x_\ell) := \int M_{\ell:u}(x_\ell, z_{\ell+1:u-1}, x_u) dz_{\ell+1:u-1}.$$

Algorithm 7 gives a pseudocode of the CPF-BBS algorithm, parameterised by a (constant) blocking sequence $1 = T_1 < \dots < T_L = T$, $T_i \in \mathbb{N}$ for all $i \in [L]$.

Algorithm 7 CPF-BBS($X_{1:T}^*, B_{1:T}; T_{1:L}$)

1: $(\underline{X}_{1:T}, \underline{A}_{1:T-1}, \tilde{B}_T) \leftarrow \text{CPF}(X_{1:T}^*, B_{1:T})$ and set $\tilde{X}_T^* \leftarrow X_T^{(\tilde{B}_T)}$
2: **for** $k = L, L-1, \dots, 2$ **do**
3: $\ell \leftarrow T_{k-1}; u \leftarrow T_k; B_u^* \leftarrow \tilde{B}_u$.
4: $B_{\ell:u-1}^* \leftarrow \text{ANCESTORTRACE}(\underline{A}_{\ell:u-1}, B_u^*)$
5: $(\tilde{X}_{\ell:u-1}^*, \tilde{B}_{\ell:u-1}) \leftarrow \text{BRIDGECPF}(\underline{X}_\ell, B_{\ell:u-1}^*, X_{\ell+1:u}^{(B_{\ell+1:u}^*)})$
6: **end for**
7: **output** $(\tilde{X}_{1:T}^*, \tilde{B}_{1:T})$

Algorithm 8 details a key element of the CPF-BBS algorithm, namely a bridging CPF which starts from an existing forward CPF state (particles), and targets a conditional distribution with the terminal value x_u^* of the block fixed.

Algorithm 8 BRIDGECPF($\underline{x}_\ell, b_{\ell:u-1}^*, x_{\ell+1:u}^*$)

1: $W_\ell^{(1:N)} \leftarrow M_{u|\ell}(x_u^* | \underline{x}_\ell)^{\frac{1}{u-\ell}}; \tilde{\mathbf{X}}_\ell \leftarrow \underline{x}_\ell$
2: **for** $v = \ell + 1 : u - 1$ **do**
3: $\tilde{A}_{v-1}^{(1:N)} \leftarrow r^{(b_{v-1}^*, b_v^*)}(\cdot | G_{v-1}(\tilde{\mathbf{X}}_{v-1}^{(1:N)}) W_{v-1}^{(1:N)})$
4: Draw $\tilde{X}_v^{(i)} \sim \bar{M}_v(\cdot | \tilde{X}_{v-1}^{(\tilde{A}_{v-1}^{(i)})}, \tilde{X}_u^*)$ for $i \neq b_v^*$ and set $\tilde{X}_v^{(b_v^*)} = x_v^*$
5: Set $\tilde{\mathbf{X}}_v \leftarrow (X_{v-1}^{(\tilde{A}_{v-1}^{(i)})}, \tilde{X}_v^{(i)})$ for $i \in \{1:N\}$.
6: $W_v^{(1:N)} \leftarrow W_{v-1}^{(\tilde{A}_{v-1}^{(1:N)})}$
7: **end for**
8: Draw $\tilde{B}_{u-1} \sim \text{Categ}(\tilde{\omega}_{u-1}^{(1:N)})$ where $\tilde{\omega}_{u-1}^{(j)} = G_{u-1}(\tilde{\mathbf{X}}_{u-1}^{(j)}) G_u(\tilde{X}_{u-1}^{(j)}, x_u^*) W_{u-1}^{(j)}$
9: $\tilde{B}_{\ell:u-2} \leftarrow \text{ANCESTORTRACE}(\tilde{A}_{\ell:u-2}, \tilde{B}_{u-1})$
10: **output** $((x_\ell^{(\tilde{B}_\ell)}, \tilde{X}_{\ell+1:u-1}^{(\tilde{B}_{\ell+1:u-1})}), \tilde{B}_{\ell:u-1})$

We record the following consistency result, ensuring the CPF-BBS is valid, whose proof is given in Appendix B:

Theorem 8. Consider Algorithm 7 as a Markov update $(X_{1:T}^*, B_{1:T}) \rightarrow (\tilde{X}_{1:T}, \tilde{B}_{1:T})$. Then, it leaves $\pi \times U(\{1:N\}^T)$ invariant.

We conclude this section with a number of remarks about Algorithm 7.

- (i) In the special case of a dense blocking sequence $T_{1:T} = 1:T$, the bridging CPF and its tracing (lines 2–7 and 9 of Algorithm 8, respectively) are eliminated, and therefore the CPF-BBS simplifies to the backward sampling CPF (CPF-BS) of [33]. This means that the CPF-BBS can be viewed as a generalisation of CPF-BS, with arbitrary blockings.
- (ii) The other extreme, that is, the trivial blocking sequence $T_1 = 1$, $T_2 = T$ leads to running a CPF and then *another* CPF with same initial particles and targeting the conditional distribution $\pi(x_{1:T-1} \mid \tilde{X}_T^*)$. This may not be practically useful, but can give insight about what the ‘bridge CPF’ is about.
- (iii) If we modify the algorithm by replacing BRIDGECPF by the following algorithm:
 - 1: Draw $\tilde{X}_{l:u-1}^{(i)}$ starting from $X_l^{(i)}$ using $\bar{M}_v(\cdot \mid \cdot, X_u^{(B_u^*)})$ for $i \neq B_u^*$.
 - 2: Set $\tilde{X}_{l:u-1}^{(B_u^*)} = X_{l:u-1}^{(B_{l:u-1}^*)}$.
 - 3: Choose $\tilde{X}_{l:u-1}^{(i)}$ with probability proportional to $M_{u|l}(\tilde{X}_u^* \mid \tilde{X}_l^{(i)}) \prod_{v=u}^{u-1} G_v(\tilde{X}_v^{(i)})$, then we get a CPF version of the extended importance sampling for particle filters suggested in [13].
- (iv) Algorithm 7 has similarities with the blocked particle Gibbs (or blocked CPF) of [30] but differs in two crucial points:
 - We suggest a block-wide ‘lookahead’ which is possible to implement thanks to Assumption 7, instead of using a modified potential only at the last time instant.
 - The block update is not conditioned on a single start point, but all particles which were generated by the ‘forward’ CPF. (Algorithm 3).

While these differences may seem technical, they can have substantial effect on the efficiency of the method. We believe that CPF-BBS often leads to more efficient algorithm in the same computational complexity, but note that the blocked particle Gibbs is directly parallelisable unlike the CPF-BBS.

7. BLOCKING SEQUENCE SELECTION

The CPF-BBS (Algorithm 7) is valid with any choice of the blocking sequence $T_{1:L}$. However, its choice affects simulation efficiency, that is, the mixing of the Markov chain. In this section, we discuss a computationally inexpensive method that can be used in practice to determine a suitable blocking sequence prior to running the CPF-BBS in order to facilitate efficient mixing.

We begin in Section 7.1 by discussing a proxy for the integrated autocorrelation time (IACT) of the Markov chain output by the CPF-BBS. Then, Section 7.2 details an estimator we have developed for the proxy. Finally, Section 7.3 describes a practical algorithm for blocking sequence selection that is based on the estimator of Section 7.2. We will study the methods presented in this section empirically in Section 9.

7.1. The probability of lower boundary updates (PLU). A theoretically attractive candidate strategy for blocking sequence selection is monitoring the IACT for variables of interest, based on the output of the CPF-BBS. Efficient inference could then be obtained by choosing the blocking sequence that minimises the IACT. However, this approach is typically computationally demanding or even infeasible, since the estimation of the IACT is notoriously difficult and often requires extensive simulation of Markov chains.

For these reasons, we base the selection of the blocking sequence on a proxy for IACT that is easier to work with. We call the proxy the ‘probability of lower boundary updates’ (PLU), and its definition for the block (ℓ, u) , using the notation of Algorithm 8, is given by

$$(7) \quad \text{PLU}(\ell, u) := \mathbb{P}(X_\ell^{(\tilde{B}_\ell)} \neq X_\ell^{(B_\ell^*)}).$$

In other words, $\text{PLU}(\ell, u)$ measures for the block (ℓ, u) the probability that the bridge CPF (Algorithm 8) updates the value at the block lower boundary ℓ . Intuitively, values of PLU close to one should be associated with low IACT, and our experiments in Section 9 support this.

7.2. Approximate estimator for the PLU. Even though $\text{PLU}(\ell, u)$ is much easier to estimate than IACT, it still requires iterating the CPF-BBS for each candidate blocking, which is computationally demanding. We have developed an estimator for $\text{PLU}(\ell, u)$ which avoids this, and is based on a single 'stationary' CPF state (the generated particles $X_{1:T}^{1:N}$ and reference indices $B_{1:T}$), which is used for any block boundaries ℓ, u . The practical algorithm postponed to Section 7.3 will be based on this idea, but assumes further that such a stationary CPF state can be well approximated by an independent particle filter.

The estimator from a single CPF state is presented in (11) below and is based on two 'asymptotic' characterisations for PLU , for small and large blocksizes, respectively. The idea behind the characterisations is that the event $X_\ell^{(\tilde{B}_\ell)} \neq X_\ell^{(b_\ell^*)}$ occurs when a trajectory traced back from the generated particle tree in the bridge CPF has a different value at the block lower boundary than the reference.

Consider first the case of a small blocksize, that is, $u - \ell \approx 1$. In this case, PLU is approximately characterised by:

$$(8) \quad \text{PLU}_M(\ell, u) := 1 - \frac{M_{u|\ell}(X_u^* | X_\ell^*)}{\sum_{j=1}^N M_{u|\ell}(X_u^* | X_\ell^{(j)})},$$

where $X_\ell^* := X_\ell^{(B_\ell)}$ and $X_u^* := X_u^{(B_u)}$ refer to the ℓ th and u th value of a reference trajectory. The rationale for (8) comes from CPF-BS being a special case of the CPF-BBS for the dense blocking with unit blocksizes. Letting b_t and b_{t+1} denote the indices of the current reference, the probability of choosing b_t in backward sampling [33] is given by:

$$\mathbb{P}(B_t = b_t | B_{t+1} = b_{t+1}) \propto w_t^{(b_t)} M_{t+1}(X_{t+1}^{(b_{t+1})} | X_t^{(b_t)}) G_{t+1}(X_t^{(b_t)}, X_{t+1}^{(b_{t+1})}).$$

Here, under the weak potential setting with approximately constant potentials, the right hand side approximately reduces to $M_{u|\ell}(X_u^{(b_u)} | X_\ell^{(b_\ell)})$ since $\ell = t, u = t + 1$ with a unit blocksize. The probability of choosing a non-reference is therefore approximately given by (8).

On the other hand, if the blocksize is large, $\text{PLU}(\ell, u)$ is approximately characterised by:

$$(9) \quad \text{PLU}_G(\ell, u) := \left(1 - \frac{1}{N}\right) \prod_{k=\ell}^{u-1} \left(1 - \frac{p_k N}{(N-1)^2}\right),$$

where the quantity p_k equals the probability that a resampling event occurs, divided by N . In the case of systematic resampling with mean partitioned weights $W_k^{(1:N)}$, (see Appendix A, Lemma 28 of [6]) and the weak potential setting, p_k may be calculated as follows (for normalised $W_k^{(1:N)}$):

$$(10) \quad p_k = \frac{1}{2} \sum_{i=1}^N \left| W_k^{(i)} - \frac{1}{N} \right|.$$

The justification of (9) comes from a calculation detailed in Appendix F, which shows that $\text{PLU}_G(\ell, u)$ approximately equals the expected proportion of particles whose ancestor at time ℓ is not the reference after an 'artificial' conditional particle system has evolved for $u - \ell$ time steps from time ℓ . Therefore, $\text{PLU}_G(\ell, u)$ maybe loosely interpreted as approximating

the probability of choosing nonreference at time ℓ , when the ancestry of a particle chosen uniformly at time u is traced back until time ℓ .

Our estimator for $\text{PLU}(\ell, u)$ is constructed by ‘interpolating’ (8) and (9) such that

$$(11) \quad \widehat{\text{PLU}}(\ell, u) := \text{PLU}_G(\ell, u) \text{PLU}_M(\ell, u) \left(1 - \frac{1}{N}\right)^{-1},$$

where the scaling is added so that the estimator approximately reduces to (8) and (9) for short and long blocks, respectively, in the weak potential setting.

The estimator in (11) was derived assuming an access to CPF state with N particles. It is also possible to estimate the $\widehat{\text{PLU}}(\ell, u)$ from a CPF (or particle filter) state which has a different number of particles N_0 (which is often useful to take ‘large’ in practice so that $N_0 \gg N$). In this case, we can estimate PLU_G and PLU_M as follows, and then use (11) with the desired N in the scaling.

To estimate PLU_G , we simply compute p_k using (10) from the N_0 particles and substitute it directly to (9) with the desired $N < N_0$. For PLU_M we use the alternative estimator of the form

$$(12) \quad \text{PLU}_M(\ell, u) = 1 - \frac{c(\ell, u)}{c(\ell, u) + N - 1},$$

which follows by assuming that

$$(13) \quad M_{u|\ell}(X_u^* | X_\ell^*) \approx c(\ell, u) M_{u|\ell}^{(T)},$$

where

$$(14) \quad M_{u|\ell}^{(T)} = \frac{1}{N_0 - 1} \sum_{j \neq B_\ell} M_{u|\ell}(X_u^* | X_\ell^{(j)}).$$

In other words, the block transition density for the reference is assumed to be approximately equal to a constant $c(\ell, u)$ times a ‘typical’ value of the block transition densities for particles not including the reference. The estimator (12) may be derived by appropriate substitution of (13) and (14) into (8).

7.3. Algorithm for blocking sequence selection. In this section we describe a practical method based on (11) to choose the blocking sequence. Algorithm 9 describes a method that uses (11) to evaluate S candidate blocking sequences $(T_{1:L^{(s)}}^{(s)})_{s=1,2,\dots,S}$ in the context of the Feynman-Kac model $(M_{1:T}, G_{1:T})$. The additional parameters N and n stand for the number of particles and number of iterations, which are tuning parameters of the blocking candidate evaluation. Here, we use indexing notation where $A[i, j, k]$ stands for the element in row i , column j and slice k in an array A . Furthermore, the columns of arrays need not have the same number of rows, and indexing operations with ‘ $:$ ’ mean ‘all elements’ in the particular dimension.

One iteration of the main loop in Algorithm 9 consists of running the standard particle filter (Algorithm 1) with mean partitioned systematic resampling followed by a traceback using ancestor tracing (Algorithm 4) in lines 2–4. Then, given the output of the particle filter, we estimate PLU using Algorithm 10 (see below) on line 5 for each block (ℓ, u) within each blocking sequence. The computation is a straightforward application of Equations (8)–(11) using the particle filtering results. Finally, lines 7–9 summarise the estimates of PLU by taking their mean over the n replicate runs of the particle filter. The element $\bar{\phi}_{\text{PLU}}[i, s]$ in the output of Algorithm 9 describes in terms of PLU, how efficient the i th block in the blocking sequence s was.

Algorithm 9 EVALUATEBLOCKINGCANDIDATES($\{T_{1:L^{(1)}}^{(1)}, \dots, T_{1:L^{(S)}}^{(S)}\}$, $M_{1:T}$, $G_{1:T}$, N , n)

```

1: for  $j = 1, \dots, n$  do
2:    $\underline{X}_{1:T}, \underline{A}_{1:T-1}, \underline{W}_{1:T} \leftarrow \text{PF}(\rho_{\text{syst}}, M_{1:T}, G_{1:T}, N)$ 
3:   Draw  $B_T \sim \text{Categ}(W_T^{(1:N)})$ 
4:    $B_{1:T-1} \leftarrow \text{ANCESTORTRACE}(A_{1:T-1}^{(1:N)}, B_T)$ 
5:    $\phi_{\text{PLU}}[:, :, j] \leftarrow \text{ESTIMATEPLU}(\{T_{1:L^{(1)}}^{(1)}, \dots, T_{1:L^{(S)}}^{(S)}\}, \underline{X}_{1:T}, \underline{W}_{1:T-1}, B_{1:T})$ 
6: end for
7: for  $s = 1, \dots, S$  do
8:   Set  $\bar{\phi}_{\text{PLU}}[i, s] = \text{MEAN}(\phi_{\text{PLU}}[i, s, :])$  for  $i = 1, \dots, L^{(s)} - 1$ .
9: end for
10: return  $\bar{\phi}_{\text{PLU}}$ 

```

Algorithm 10 ESTIMATEPLU($\{T_{1:L^{(1)}}^{(1)}, \dots, T_{1:L^{(S)}}^{(S)}\}$, $\underline{X}_{1:T}, \underline{W}_{1:T-1}, B_{1:T}$)

```

1: Compute  $p_k$  for  $k = 1, \dots, T - 1$  using (10).
2: for  $s = 1, \dots, S$  do
3:   for  $i = 1, \dots, L^{(s)} - 1$  do
4:     Set  $\ell = T_i^{(s)}; u = T_{i+1}^{(s)}$ ;
5:     Set  $X_{\ell}^{*} = X_{\ell}^{(B_{\ell})}; X_u^{*} = X_u^{(B_u)}$ ;
6:     Compute  $\text{PLU}_M(\ell, u)$  using (8).
7:     Compute  $\text{PLU}_G(\ell, u)$  using (9).
8:     Compute  $\widehat{\text{PLU}}(\ell, u)$  using (11).
9:     Set  $\phi_{\text{PLU}}[i, s] = \widehat{\text{PLU}}(\ell, u)$ .
10:   end for
11: end for
12: return  $\phi_{\text{PLU}}$ 

```

Algorithm 9 may in principle be used to evaluate any blocking sequence, but we suggest to use it with Algorithm 13 given in Appendix E.2 that constructs blocking sequences where the blocksizes $T_{k+1} - T_k$ are powers of two. More precisely, if $T = 2^{p^*} + 1$ for some p^* , Algorithm 13 returns blocking sequences $T_{1:L^{(i)}}^{(i)}$ for $i = 1, 2, \dots, p^* + 1$, where the blocksizes of the i th sequence are all constant 2^{i-1} . If $T \neq 2^{p^*} + 1$, similar sequences are returned, but with a possible ‘residual block’ of length $< 2^{i-1}$ as the last block in each sequence i .

Finally, Algorithm 11 describes a method based on Algorithms 9 and 13 for choosing a single blocking sequence to be used with the CPF-BBS and a given Feynman-Kac model. In summary, Algorithm 11 first constructs the candidate blocking sequences using Algorithm 13. Then, Algorithm 9 is run to obtain $\bar{\phi}_{\text{PLU}}$ given these sequences. The data $\bar{\phi}_{\text{PLU}}$ is then reinterpreted as a set of elements D_{PLU} , whose element (ℓ, b, p) describes the estimated PLU, p , of the block with lower boundary ℓ and upper boundary $\ell + b$. Finally, D_{PLU} is processed such that blocking sequences with largest blocksizes are considered first, and at each block lower boundary, the best performing blocksize in terms of the estimated PLU is selected to the output blocking sequence.

Algorithm 11 CHOOSEBLOCKING($M_{1:T}, G_{1:T}, N, n$)

```

1:  $\{T_{1:L^{(1)}}^{(1)}, \dots, T_{1:L^{(p)}}^{(p)}\} \leftarrow \text{DYADICCANDIDATEBLOCKINGS}(T)$ 
2:  $\bar{\phi}_{\text{PLU}} \leftarrow \text{EVALUATEBLOCKINGCANDIDATES}(\{T_{1:L^{(1)}}^{(1)}, \dots, T_{1:L^{(p)}}^{(p)}\}, M_{1:T}, G_{1:T}, N, n)$ 
3: Compute  $D_{\text{PLU}}$ , a container with elements of the form  $(\ell, b, p)$  based on  $\bar{\phi}_{\text{PLU}}$ .
4: Initialise  $D$ , an empty container for elements of the form  $(\ell, b)$ .
5: for  $s = p, p-1, \dots, 1$  do
6:   Get lower boundaries and blocksizes  $(\ell_k, b_k)$  for  $k = 1, \dots, L^{(s)} - 1$  from  $T_{1:L^{(s)}}^{(s)}$ .
7:   for  $k = 1, \dots, L^{(s)} - 1$  do
8:     Denote by  $D_{\text{PLU}}^{(\ell_k)}$  all elements of  $D_{\text{PLU}}$  whose block lower boundary equals  $\ell_k$ .
9:     if maximal  $p$  is reached when blocksize equals  $b_k$  among elements of  $D_{\text{PLU}}^{(\ell_k)}$  then
10:      Add  $(\ell_k, b_k)$  to  $D$ .
11:      Remove all elements of  $D_{\text{PLU}}$  with  $\ell$  such that  $\ell_k \leq \ell < \ell_k + b_k$ .
12:    end if
13:   end for
14: end for
15: return Blocking sequence constructed from elements of  $D$ .

```

8. APPLICATION TO DISCRETISED LINEAR DIFFUSIONS WITH PATH INTEGRAL WEIGHTS

We discuss next a class of continuous-time models and their discretisations, for which the methods of Section 6–7 are particularly useful. We will consider instances of these models also in the experiments (Section 9).

We start with the continuous-time model on a time interval $[0, \tau]$. The prior dynamics \mathbb{M} correspond to the solution of a linear stochastic differential equation (SDE):

$$(15) \quad dX_t = \mathbf{F}X_t dt + \mathbf{K}dB_t, \quad X_0 \sim N(\mu_{\text{init}}, \Sigma_{\text{init}})$$

where \mathbf{B}_t is a d -dimensional Brownian motion and \mathbf{F} and \mathbf{K} are matrices of appropriate dimension, and μ_{init} and Σ_{init} are the mean and covariance of the initial distribution, respectively. The law of interest is \mathbb{M} weighted by non-negative weights of the form

$$w(x_{[0,\tau]}) = \exp \left(- \int_0^\tau V(x_u) du \right),$$

where $V : \mathbb{X} \rightarrow [0, \infty]$ are ‘potential’ functions that ‘penalise’ the trajectories of \mathbb{M} . That is, the distribution of interest is proportional to $\mathbb{M}(dx_{[0,\tau]})w(x_{[0,\tau]})$.

In practice, we assume a time discretisation of $[0, \tau]$:

$$(16) \quad 0 = t_1 < t_2 < \dots < t_T = \tau,$$

which leads to the discrete-time FK-model (1).

The dynamics $M_{1:T}$ in (1) correspond to the marginals of $X_{[0,\tau]} \sim \mathbb{M}$, that is:

$$(17) \quad \begin{aligned} M_1 &= \text{Law}(X_{t_1}) = N(\mu_{\text{init}}, \Sigma_{\text{init}}) \\ M_k(\cdot \mid x) &= \text{Law}(X_{t_k} \mid X_{t_{k-1}} = x) \quad \text{for } 2 \leq k \leq T, \end{aligned}$$

which are linear-Gaussian. Appendix C details how M_k can be derived from the parameters of the SDE, and also how their necessary conditional distributions required by Assumption 7 can be determined.

The potential functions $G_{1:T}$ in (1) stem from approximating the path integral by a Riemann sum:

$$(18) \quad w(x_{[0,\tau]}) = \prod_{k=1}^{T-1} \exp \left(- \int_{t_k}^{t_{k+1}} V(x_u) du \right) \approx \prod_{k=1}^{T-1} \exp \left(- |\Delta_k| V(x_{t_k}) \right),$$

where $\Delta_k = [t_k, t_{k+1})$ and $|\Delta_k| = t_{k+1} - t_k$. This leads to potentials of the following form:

$$(19) \quad \begin{aligned} G_1(x_{t_1}) &= \exp \left(- (t_2 - t_1) V(x_{t_1}) \right) \\ G_k(x_{t_{k-1}}, x_{t_k}) &= \exp \left(- (t_{k+1} - t_k) V(x_{t_k}) \right) \quad \text{for } 2 \leq k \leq T-1 \\ G_T &\equiv 1. \end{aligned}$$

Remark 9. The scenario detailed above can be generalised and/or modified in a number of ways. Indeed, the potentials G_k can also include purely discrete-time elements, as in our Cox process experiment (Section 9.2).

The law \mathbb{M} , or equivalently M_k , can also correspond to the law of linear SDE *conditioned on* a number of linear-Gaussian observations. In such a case, the distributions M_k are still linear-Gaussian, and we can derive the required conditional laws. This can be useful in many practical settings, and indeed was essential for our movement model example (Section 9.3).

9. EXPERIMENTS

9.1. Comparing conditional resamplings with Algorithm 7. We first investigate the performance of the CPF-BBS (Algorithm 7) using the conditional resamplings ρ_{kill} and ρ_{syst} . For reference, we also study conditional multinomial resampling with conditioning indices i and k , $\rho_{\text{mult}}^{(i,k)}$. This conditional resampling may be simply implemented by first drawing the ancestor indices $A^{(1:N)} \sim \text{Categ}(w^{(1:N)})$ as in standard multinomial resampling, and then enforcing the condition $A^{(k)} = i$.

In this section, we study a correlated random walk incorporating a path integral type potential function, hereafter called the CTCRW-P model. The dynamics of the model $X_t = (V_t \ L_t)^T$ are driven by the stochastic differential equation (SDE)

$$(20) \quad \begin{aligned} dV_t &= -\beta_v V_t dt + \sigma dB_t \\ dL_t &= [-\beta_x L_t + V_t] dt, \end{aligned}$$

where B_t is the standard Brownian motion, σ , β_v and β_x are parameters, and $(L_t)_{t \geq 0}$ and $(V_t)_{t \geq 0}$ represent location and velocity processes, respectively. The potential function is

$$(21) \quad \exp \left(- \int_0^\tau \frac{L_u^2}{2\eta^2} du \right) = \prod_{k=1}^{T-1} \exp \left(- \int_{t_k}^{t_{k+1}} \frac{L_u^2}{2\eta^2} du \right),$$

where η is a parameter and the discretisation points are defined as in (16). The Feynman-Kac representation (17) & (19) is completed for CTCRW-P by setting:

$$(22) \quad \begin{aligned} M_1 &:= N(0, S), \\ M_k(\cdot \mid x) &:= N(T_{t_{k-1}, t_k} x, Q_{t_{k-1}, t_k}), \quad \text{for } 2 \leq k \leq T, \\ V(X_t) &:= \frac{L_t^2}{2\eta^2}, \end{aligned}$$

where T_{t_{k-1}, t_k} , Q_{t_{k-1}, t_k} and S are the transition matrix, conditional covariance matrix and stationary covariance matrix, respectively, arising in the solution of the linear SDE (20).

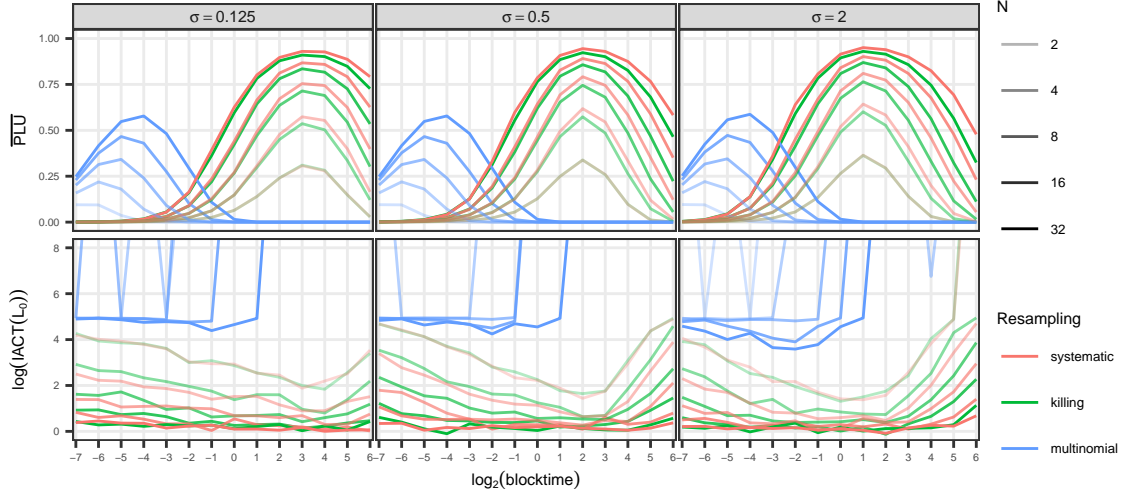


FIGURE 1. The estimated mean probability of lower boundary updates and the logarithm of the integrated autocorrelation time with varying σ for the location state variable at time 0.0 in the CTCRW-P model. The colors correspond to systematic, killing and multinomial resamplings, respectively. The transparency of the lines indicates the number of particles used. The horizontal axis gives the value of the blocktime, as described in the text. The value of $|\Delta_k|$ was set to 2^{-7} . The performance of CPF-BS is seen at the far left, with blocktime = 2^{-7} .

Their expressions are given in Appendix D.1, in Equations (47), (48)–(49) and (50)–(51), respectively.

We ran the CPF-BBS targetting (22) with the configurations $N \in \{2, 4, 8, 16, 32\}$, $\text{blocktime} \in \{2^{-7}, 2^{-6}, \dots, 2^6\}$ and $r \in \{\rho_{\text{syst}}, \rho_{\text{kill}}, \rho_{\text{mult}}\}$. Here, blocktime parameterises the blocking sequence in terms of the ‘physical time’ of the discretised SDE. The blocksizes $T_{k+1} - T_k$ in Algorithm 7, may simply be obtained by dividing blocktime by $|\Delta_k|$ (see below). For each run of the CPF-BBS, we used 21000 iterations with the first 1000 discarded as burnin.

In model (22), we set $\tau = 2^6$, $|\Delta_k| = 2^{-7}$, $\eta = 1.0$ and $\sigma \in \{0.125, 0.5, 2.0\}$, which controls the variability in the velocity process. Each time, given σ , we solved for the parameters β_x and β_v such that the stationary covariance matrix (50) had unit variances on the diagonal. This was done to ensure that the variability of the process remains similar as σ changes.

The simulations were run with all combinations of the algorithm and model configurations described above. We estimated PLU (discussed in Section 7.1) by tallying iterations where $x_\ell^{(\tilde{B}_\ell)} \neq x_\ell^{(b_\ell^*)}$ and dividing by their total, and estimated the IACT for $L_{0.0}$ using batch means [17]. Figure 1 summarises the results of this experiment. The mean PLU shown in the top row is computed over the number of blocks (given here by $\tau/\text{blocktime}$). The figure shows systematic and killing resampling performing better than multinomial resampling, which can be seen from the lower IACTs and higher mean PLU. The performance with multinomial resampling is poor here, as expected, since the model has weak potentials with $|\Delta_k| = 2^{-7}$. In contrast, killing and systematic resampling behave nearly uniformly, with systematic resampling performing slightly better. This finding aligns well with the theoretical and empirical findings in [6] for the particle filter in a similar context of path integral potentials and $|\Delta_k|$ close to 0.

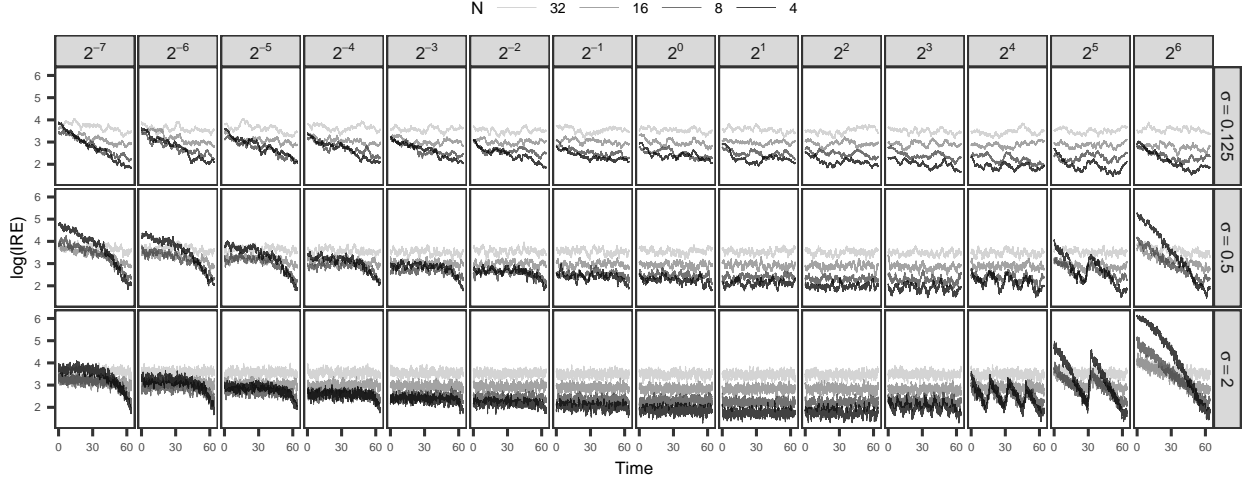


FIGURE 2. The logarithms of inverse relative efficiency obtained at each time-point with conditional systematic resampling in the experiment discussed in Section 9.1. The columns show the results with varying blocktime in Algorithm 7.

The CPF-BBS coincides with the CPF-BS when blocktime = $|\Delta_k|$, which corresponds to the first value on the horizontal axis. Even though increasing N naturally improves the performance of the CPF-BS too, the CPF-BBS has better simulation efficiency with an appropriately chosen blocktime, for any N in the simulation. Note that the estimation of the IACT is quite noisy here, since the mixing is poor especially with multinomial resampling and with poorly chosen blocking sequences induced by the value of blocktime. In contrast, the computed mean PLU appears less noisy, and in the case of systematic and killing resampling the best blocktime in terms of IACT is identified.

We also investigated the relationship of PLU with IACT_{32,0}, and the findings were similar. A further experiment fixing $\sigma = 1.0$ and varying $\eta \in \{0.125, 0.5, 2.0\}$ instead also resulted in similar findings (see supplementary Figure 8).

9.2. Choice of the blocking sequence. As already illustrated empirically with Figure 1 and discussed in Section 7, the choice of the blocking sequence is a tuning parameter affecting the sampling efficiency of the CPF-BBS. Figure 2 exemplifies this further by showing another look at the results obtained from the experiment in the previous section. Here, the logarithm of the inverse relative efficiency (IRE) is plotted at each timepoint when systematic resampling was used. The IRE is obtained by scaling the IACT by the number of particles, and measures the asymptotic efficiencies of estimators with varying computational costs [18]. The panes from left to right show the results with varying blocktime and represent a range of algorithms from the CPF-BS (blocktime = 2^{-7}) to an algorithm similar to running the CPF twice (blocktime = 2^6). The optimal algorithms use only 4 particles, motivating the search for an appropriate blocktime (or blocking sequence). By visual inspection, it appears the optimal blocktimes here are around $2^1 - 2^2$ for $\sigma = 2.0$, $2^2 - 2^3$ for $\sigma = 0.5$ and $2^3 - 2^4$ for $\sigma = 0.125$. Here, a decrease in the value of σ results in a larger optimal blocktime, since decreasing σ leads to increased ‘stiffness’ in the dynamics of $M_{1:T}$. The optimal blocktimes represent balances where the blocks are large enough so that bridging between the lower and upper boundaries is sufficiently likely, and small enough so that degeneracy of the particle tree within the block is avoided.

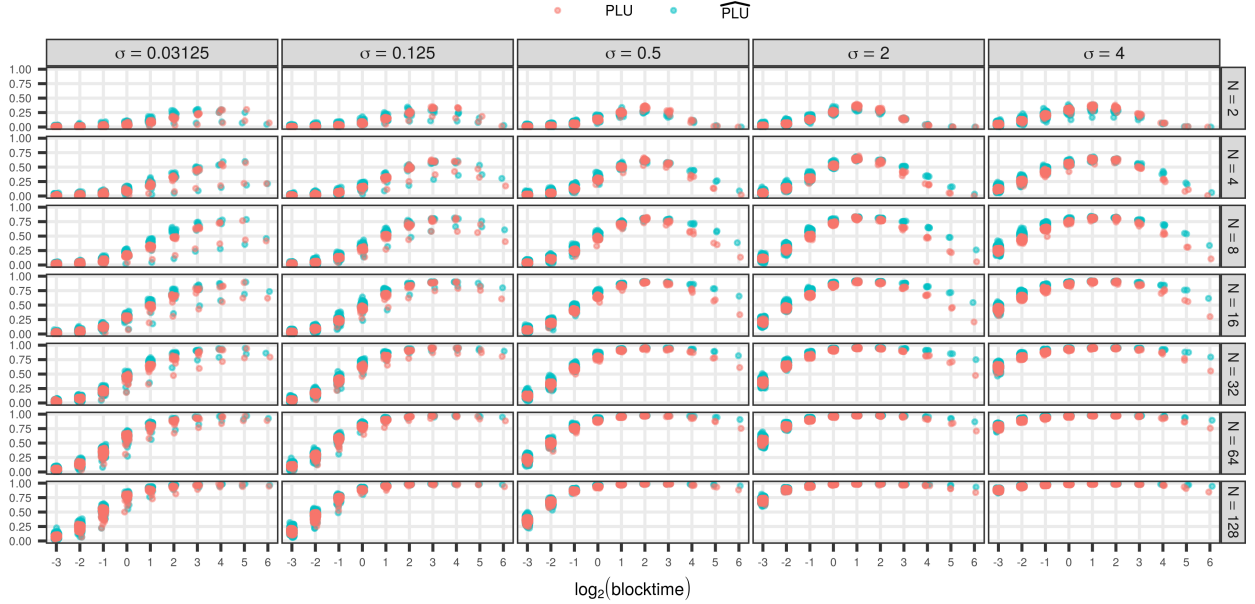


FIGURE 3. The PLU (orange) and $\bar{\phi}_{PLU}$ (light blue) for each block induced by the blocktime on the horizontal axis in the experiment discussed in the text for the CTCRW-P model. Slight horizontal jitter has been added to the points visualised.

Next, we investigate how well the estimates of $\bar{\phi}_{PLU}$ computed using Algorithm 9 coincide with the true PLU. We studied the relationship of $\bar{\phi}_{PLU}$ and PLU with respect to blocktime (that is, with blocking sequences constructed with constant blocksizes) using the CTCRW-P model (22) with $N \in \{2^1, 2^2, \dots, 2^{10}\}$ and the parameter $\sigma \in \{0.03125, 0.125, 0.5, 2, 4\}$. The rest of the model configuration was as in Section 9.1. Each time, to get an estimate of the true PLU, we ran 1100 iterations of Algorithm 7 with the first 100 discarded burnin, monitoring for each block the proportion of iterations where $x_\ell^{(\tilde{B}_\ell)} \neq x_\ell^{(b_\ell^*)}$. In Algorithm 9, we used $n = 50$ runs of the particle filter and N as reported above. Figure 3 visualises the results for $N \leq 2^7$ (the results for $N > 2^7$ yield no further conclusions). The true and estimated PLU appear to be in close agreement, with only slight discrepancies seen for large blocktimes. This finding motivates the use of $\bar{\phi}_{PLU}$ as a maximisation criterion for finding a blocksize that likely results in a high overall PLU as well.

Next, we turned to study Algorithm 11 for selecting the blocking sequence based on $\bar{\phi}_{PLU}$. We investigated this with a model that slightly differs from the form (19), and is a Cox process model incorporating a reflected Brownian motion (CP-RBM) first appearing in [6] and briefly detailed (with minor changes) below.

The CP-RBM model assumes an inhomogeneous Poisson process (IPP) in time, generating observation sequences $\tilde{\tau}$. The intensity function of the IPP is piecewise constant, and given by

$$(23) \quad \lambda(t) = \beta \exp(-\alpha X_{t_k}), \quad \text{for } t \in [t_k, t_{k+1}).$$

The process $(X_{t_k})_{k=1, \dots, T}$ is distributed such that

$$(24) \quad \begin{aligned} X_{t_1} &\sim N^{(r)}(0, 1, a, b) \\ X_{t_k} \mid X_{t_{k-1}} = x_{t_{k-1}} &\sim N^{(r)}(x_{t_{k-1}}, |\Delta_k| \sigma^2, a, b), \end{aligned}$$

where $N^{(r)}(\mu, \sigma^2, a, b)$ is a distribution we call the ‘reflected normal distribution’, with parameters μ , σ and bounds a and b . To simulate from $N^{(r)}(\mu, \sigma^2, a, b)$, one first draws $Z \sim N(\mu, \sigma^2)$ and then sets $X = \text{reflect}(Z, a, b)$, where ‘reflect’ is an operation that recursively reflects (that is, mirrors over a boundary) Z with respect to a (if $Z < a$) or b (if $Z > b$) until a value within (a, b) is obtained and outputted.

To apply the CPF-BBS with the CP-RBM, we use the following Feynman-Kac representation that differs from that of [6] such that the reflection of the process X is accounted for in the potential functions:

$$\begin{aligned}
 M_1 &:= N(0, 1) \\
 M_k(\cdot | x) &:= N(x, |\Delta_{k-1}| \sigma^2), \text{ for } 2 \leq k \leq T \\
 (25) \quad G_1(x) &:= \frac{N^{(r)}(x; 0, 1, a, b) \exp(-|\Delta_1| \beta \exp(-\alpha x))}{N(x; 0, 1)} (\beta \exp(-\alpha x))^{\mathbf{1}(\exists i \text{ s.t. } \tilde{\tau}_i \in \Delta_1)} \\
 G_k(x, y) &:= \frac{N^{(r)}(y; x, |\Delta_{k-1}| \sigma^2, a, b) \exp(-|\Delta_k| \beta \exp(-\alpha y))}{N(y; x, |\Delta_{k-1}| \sigma^2)} \times \\
 &\quad (\beta \exp(-\alpha y))^{\mathbf{1}(\exists i \text{ s.t. } \tilde{\tau}_i \in \Delta_k)}, \text{ for } 2 \leq k \leq T
 \end{aligned}$$

where $|\Delta_T| = 0$. This Feynman-Kac model is valid for the inference of the CP-RBM in the situation that the time discretisation is made fine enough such that each Δ_k contains at most one observation. The density $N^{(r)}(x; \mu, \sigma^2, a, b)$ contains an infinite sum, which we truncate to the first ten terms; the formula is given in Appendix D.2.

We first drew a realisation of the process X using (24) with $|\Delta_k| = 2^{-6}$, $\sigma = 0.3$, $a = 0$, $b = 3$ and time interval length $\tau = 2^8$. Then, conditional on this realisation, we simulated one dataset, $\tilde{\tau}$, from the IPP defined by (23) with $\alpha = 1$ and $\beta = 0.5$. Finally, we refined the time discretisation such that (25) could be used.

For the blocking sequences, we considered the sequences induced by the constant block-times $\{2^{-6}, 2^{-5}, \dots, 2^5\}$ and a (nonhomogeneous) blocking sequence constructed using Algorithm 11 with $n = 50$ and $N = 8$. Here, a minor change to the choice of candidate blockings (that is, Algorithm 13) was done: instead of constructing them using blocksizes (integers) in powers of two as discussed in Section 7, we constructed them using the power of two blocktimes $2^{-6} - 2^5$ as this is more natural for a continuous-time model. For each blocking sequence, we then applied the CPF-BBS with $N = 8$ for 26000 iterations with the first 1000 discarded as burnin.

Figure 4 summarises the results of the experiment. The top pane shows the true simulated state, the observations $\tilde{\tau}$ and the 50% and 95% probability intervals of the distributions $X_t | \tilde{\tau}$ for $t \in t_1, t_2, \dots, t_T$. The middle pane compares the IACTs obtained from the samples of said distributions with the different blocking strategies; the nonhomogeneous blocking is highlighted in red. The IACTs for the blocking sequences constructed for blocktimes $> 2^3$ were greater than for the depicted blocking strategies. Finally, the bottom pane visualises the nonhomogeneous blocking sequence obtained using Algorithm 11.

In terms of the IACT the blocking sequence returned by Algorithm 11 appears to perform similarly to the best choices for the blocking sequences constructed with constant block-times, indicating that the method here provides adequate performance without trial runs of the CPF-BBS. The bottom pane shows how the blocktime of the nonhomogeneous blocking switches between $1/2, 1$ and 2 .

9.3. Movement modelling with noisy observations and terrain preference. We conclude with an application of the CPF-BBS to a movement modelling scenario. Here, we are interested in modelling the movement of an object on a plane based on noisy observations

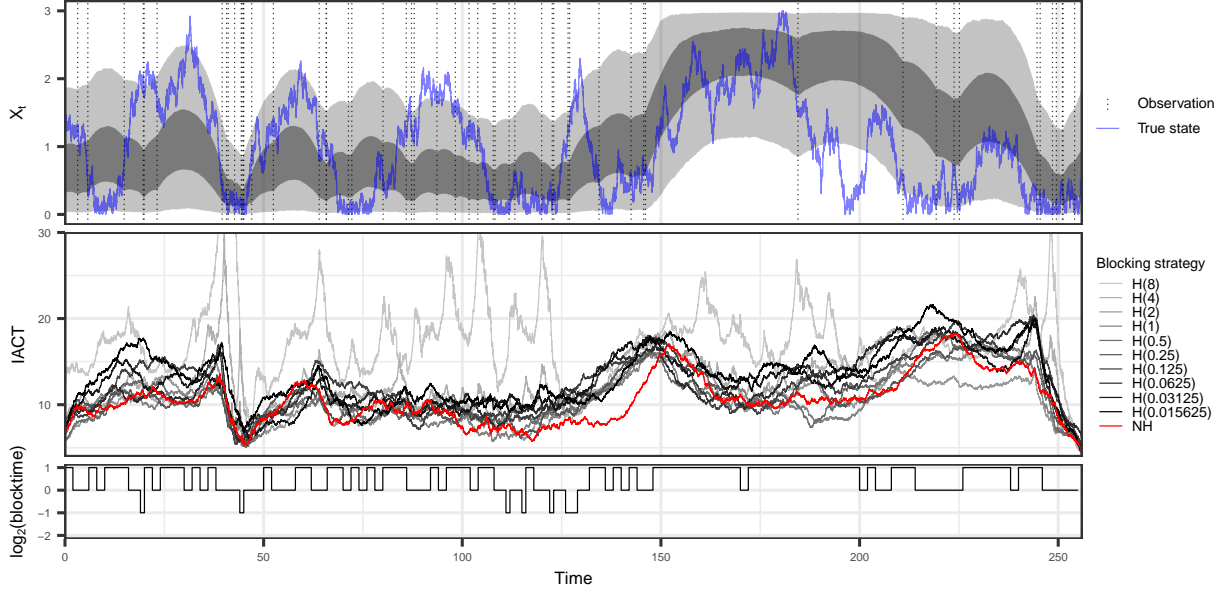


FIGURE 4. Top: the observations $\tilde{\tau}$ (dotted vertical lines) and the 50% and 95% probability intervals for $X_t | \tilde{\tau}$. The true simulated state is shown in blue. Middle: the integrated autocorrelation times obtained with homogeneous blocking sequences parameterised by blocktime $\leq 2^3$ (shades of gray), and with the nonhomogeneous blocking sequence in the bottom plot (red). In the legend, $H(x)$ refers to the blocking sequence induced by constant blocktime x , and NH stands for the nonhomogeneous blocking. Bottom: the nonhomogeneous blocking sequence obtained by running Algorithm 11 using $n = 50$ and $N = 8$ for the CP-RBM model as discussed in the text.

and knowledge of terrain in which the object moves. We assume that the object has a ‘preference’ for spending time in certain types of terrain.

To model such a setting, we build on the continuous-time correlated random walk (CTCRW) model developed for animal movement modelling based on telemetry data [21]. The dynamics of the CTCRW model arise from a special case of the SDE (20), obtained by setting $\beta_x = 0$ and denoting $\beta := \beta_v$. Using this SDE independently in x and y dimensions yields a 4-dimensional state $X_t = (V_t^{(x)}, L_t^{(x)}, V_t^{(y)}, L_t^{(y)})^T$ and a movement model on the plane, which we call the CTCRW SDE. The full CTCRW model also incorporates two-dimensional location observations $y = (y_k)_{k=1,2,\dots,K_y}$ observed at times $(\tilde{t}_k)_{k=1,2,\dots,K_y}$. Each observation is related to the location state variables, $\mathbf{L}_t = (L_t^{(x)}, L_t^{(y)})^T$, with

$$(26) \quad y_k = \mathbf{L}_{\tilde{t}_k} + \epsilon_k,$$

where $\epsilon_k \sim N(0, \eta^2 I_2)$, where η is a standard deviation and I_2 stands for the 2×2 identity matrix. We use the initial distribution $X_{t_1} \sim N((0, y_{11}, 0, y_{12})^T, \text{diag}(\sigma_V^2, \sigma_L^2, \sigma_V^2, \sigma_L^2))$, where y_{11} and y_{12} are the first and second coordinates of the first observation, respectively, $\sigma_V^2 = \sigma^2/(2\beta)$ (the stationary variance of the velocity component) and σ_L^2 is a parameter. The details regarding the solution of the CTCRW SDE are given in Section D.3.

Our model, which we denote CTCRW-T (T standing for ‘terrain’) differs from the CTCRW model of [21] by incorporating the effect of terrain. We use a discretisation of the CTCRW SDE conditioned on the observations as the sequence of M_k ’s in the Feynman-Kac representation of the CTCRW-T. More specifically, we use time discretisation (16) and

define

$$(27) \quad \begin{aligned} M_1 &= \text{Law}(X_{t_1} \mid Y = y), \\ M_k(\cdot \mid x) &= \text{Law}(X_{t_k} \mid X_{t_{k-1}} = x, Y = y), \quad \text{for } 2 \leq k \leq T, \end{aligned}$$

where X_t stands for the state of the CTCRW model at time t and Y stands for all observations and y their realised values. The distributions in (27) are Gaussian, and their computation can be carried out by very similar conditioning as discussed in Appendix C.

The CTCRW-T models terrain preference through its potential that is of the form (18) with the function V defined as:

$$(28) \quad V(x) = -\log(v_i), \quad \text{when } x \text{ is in terrain } i.$$

Here, $v_i \in [0, 1]$, $i = 1, \dots, K_T$, are values we call ‘terrain coefficients’, which induce the potential values for each of the K_T terrain types.

We apply the CTCRW-T model in a region of Finland containing lakes, plotted in the background of Figure 5. The colors of the background map depict the value of V , with black representing larger values, that is, lower potential. The terrain types are defined based on the Corine Land Cover classification [16] which classifies each 20×20 metre cell in Finland to one of five classes. The terrain types and terrain coefficients we use are given in Table 1. Here, we set the terrain coefficient of water bodies to zero, since we want to constrain the movement on land only.

With the potential map constructed this way, we set $\tau = 16$ and handpicked 16 observed locations in a clockwise pattern around the lakes, spacing the observation times equidistantly in time. The observed locations appear as crosses in Figure 5. The CTCRW model parameters β and σ were fit via maximum likelihood, and we set $\eta = 50$ and $\sigma_L = 50$.

We then applied the CPF-BBS with systematic resampling, $N = 16$ and blocktime = 1.0 for 11000 iterations, discarding the first 1000 as burnin. $|\Delta_k|$ was set to 2^{-7} . The right pane of Figure 5 shows 250 of the simulated location trajectories from the CTCRW-T model. In comparison, the left pane shows trajectories simulated from the CTCRW model conditioned on the observed locations, simulated using (27). We observe that the trajectories simulated from the CTCRW-T model are influenced by the conditioning on the observations, while avoiding water bodies, as desired.

We also tested the performance of the CPF-BBS with the blocking sequence obtained using Algorithm 11 (using $N = 512$ and $n = 25$), as well as CPF-BS in this example. Here, the number of particles for Algorithm 11 had to be set slightly higher to ensure that a sufficient number of particles end up in regions of positive potential (due to the hard constraint induced by ‘water bodies’). Figure 6 compares the three algorithms by plotting the IACT of the state variable $L_t^{(x)}$ with respect to time. The plots for the other state variables were similar. Clearly, the simulation efficiencies of both variants of the CPF-BBS are superior here in comparison to the CPF-BS. Between the optimised blocking and constant blocking, the finding is similar as with the CP-RBM model: the blocking optimisation via Algorithm 11 yields similar results as the ‘hand tuned’ constant blocking with blocktime = 1.0. The supplementary material also includes an animation that visualises the values of all sampled trajectories at each timepoint of the simulation, showing slower exploration of the target distribution using the CPF-BS.

We also experimented with the three algorithms using a higher value for $|\Delta_k|$, a situation where a greater discretisation error in the approximation (18) may be tolerated. We found that when $|\Delta_k|$ was increased to 0.125, the resulting IACTs of $L_t^{(x)}$ were similar between the three algorithms (see Figure 7 in the supplementary material).

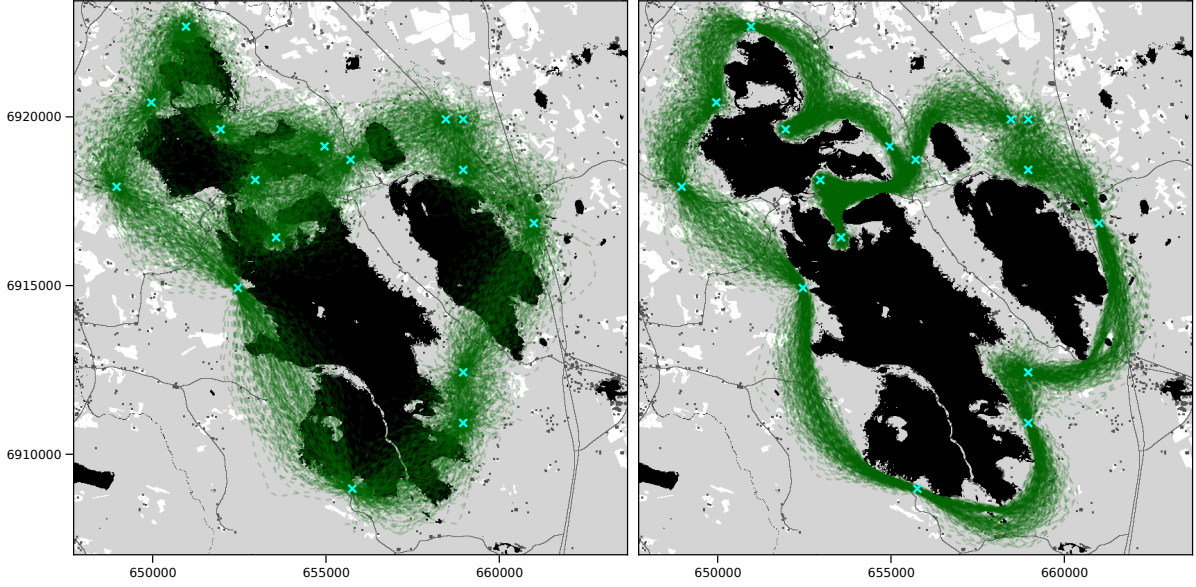


FIGURE 5. A comparison between the CTCRW and CTCRW-T models using 250 simulated location trajectories in a terrain with lakes and various types of land. The noisy observed locations are marked with crosses. The left pane shows the trajectories simulated from the CTCRW movement model conditioned on the observed locations. The right pane shows the trajectories simulated from the CTCRW-T model, which additionally incorporates the terrain preference to the conditioned CTCRW process.

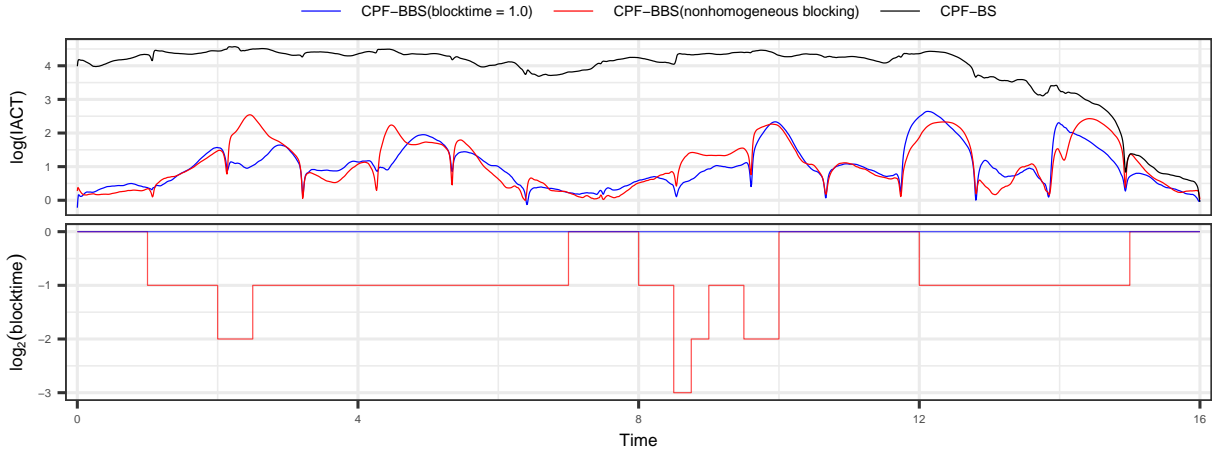


FIGURE 6. Top: The logarithm of the integrated autocorrelation time of the state variable $L_t^{(x)}$ in the CTCRW-T model when the simulation discussed in the text was run with $|\Delta_k| = 2^{-7}$ using the CPF-BS and the CPF-BBS with blocktime 1.0 and the blocking sequence found using Algorithm 11. Bottom: the blocking sequences used in the variants of the CPF-BBS.

TABLE 1. The terrain types and terrain coefficients used with the CTCRW-T model.

Terrain type	Terrain coefficient (v_i)
Artificial surfaces	0.2
Agricultural areas	0.6
Forests and semi-natural areas	0.5
Water bodies	0.0
Wetlands	0.5

10. DISCUSSION

The methods presented in this paper make inference more efficient (and feasible) for an important class of statistical models, which includes hidden Markov models (HMMs) involving weakly informative observations and, in particular, time-discretisations of continuous-time path integral models.

Our first contribution was presenting two new conditional resampling algorithms for CPFs in such a context: the killing resampling ρ_{kill} , and the systematic resampling with mean partitioned weights ρ_{syst} . Our empirical experiments with the developed resampling algorithms revealed that ρ_{syst} performs slightly better than ρ_{kill} , coinciding with the recent findings of [6] for the standard particle filter in a similar context. Based on our findings, we recommend to use ρ_{syst} with the CPF in the weak potential regime.

Our main contribution is a new CPF, which we call the conditional particle filter with bridge backward sampling (CPF-BBS), which may be regarded as a generalisation of the celebrated CPF with backward sampling (CPF-BS) [33]. The key ingredient of the CPF-BBS which avoids performance issues of the CPF-BS in the weak potentials context, is the bridging CPF step that updates the latent trajectory subject to a blocking sequence that acts as a tuning parameter of the method. Since tuning the blocking sequence by ‘trial and error’ is laborious and costly, we presented a computationally cheap procedure for finding an appropriate blocking sequence. The procedure is based on a proxy of the integrated autocorrelation time of the output Markov chain, the so-called probability of lower boundary updates (PLU), which measures the probability that the bridge CPF updates the value at the block lower boundary. We derived an estimator for PLU that we suggest to use for blocking sequence tuning via Algorithm 11 that uses a small number of trial runs of the standard particle filter with ancestor tracing to estimate PLU prior to running the CPF-BBS.

The CPF-BBS is generally applicable, assuming that the conditional distributions $M_{u|\ell}$ and $M_{k|k-1,u}$ related to the individual blocks (ℓ, u) and the dynamics $M_{1:T}$ may be computed. This may seem restrictive, but it is important to note that M_k need not necessarily correspond to the model, but may be any ‘proposal’ distributions satisfying Assumption 7. Careless choice of M_k might however result in informative potentials G_k and therefore poor performance. The contrary is also possible: with suitably chosen M_k , the G_k can be weakly informative, even if the HMM observations are informative. This can be achieved by designing M_k by suitable ‘lookaheads’ [19], such as an approximate smoothing distribution from a Laplace approximation [cf. 32, Section 8.1].

The experiments suggested that our estimator for PLU is in good agreement with the true PLU. Algorithm 11, which finds an appropriate blocking automatically, showed promising behaviour in our experiments, leading to performance similar to ‘hand tuning’ the blocking sequence. Using Algorithm 11 is easy: it only requires the user to specify the number of iterations and number particles used in the selection to obtain adequate performance ‘out of the box’. In all of the examples we studied, we found 50 iterations to suffice for block

selection, but we presume that the number of particles has to be chosen in a model by model basis.

The performance of the CPF-BBS in practice was promising: we found that the method can provide a substantial performance improvement over CPF-BS in the weak potential setting. This was particularly clear with our movement modelling experiment, which can be of independent interest for certain applications.

We believe that PLU and the ideas in the estimator we derived for it can be of interest in other contexts, too. In Section 7.2 we discussed the possibility of obtaining estimates for PLU for $N \neq N_0$, where N_0 is the number of particles used for the necessary computations. We found empirically (results not reported) that the agreement between PLU and $\widehat{\text{PLU}}$ remains similar as in Figure 3 if we use this alternative estimation procedure. This method could potentially be elaborated to a heuristic for choosing the number of particles N for the CPF-BBS. One potential way forward is to determine a ‘cutoff level’ for how large a PLU is ‘large enough,’ and the smallest N reaching this level would be chosen. However, further developments of these ideas are out of the scope of the present paper.

Finally, we note that in some applications relevant for the weakly informative context, the initial distribution M_1 can be diffuse (relative to the smoothing distribution) — even an (improper) uniform measure. In such a case, the CPF and also the CPF-BBS will suffer from poor mixing, but there are relatively direct extensions that are applicable also with the CPF-BBS. Indeed, [15] discuss general state augmentations that can be useful, and a straightforward implementation is often possible in terms of M_1 -reversible transitions [22].

ACKNOWLEDGEMENTS

SK and MV were supported by Academy of Finland project 315619 and the Finnish Centre of Excellence in Randomness and Structures.

REFERENCES

- [1] C. Andrieu, A. Doucet, and R. Holenstein. Particle Markov chain Monte Carlo methods. *J. R. Stat. Soc. Ser. B Stat. Methodol.*, 72(3):269–342, 2010.
- [2] C. Andrieu, A. Lee, and M. Vihola. Uniform ergodicity of the iterated conditional SMC and geometric ergodicity of particle Gibbs samplers. *Bernoulli*, 24(2):842–872, 2018.
- [3] M. Arnaudon and P. Del Moral. A duality formula and a particle Gibbs sampler for continuous time Feynman-Kac measures on path spaces. *Electron. J. Probab.*, 25:1–54, 2020.
- [4] C. K. Carter, E. F. Mendes, and R. Kohn. An extended space approach for particle Markov chain Monte Carlo methods. Preprint arXiv:1406.5795, 2014.
- [5] N. Chopin and S. S. Singh. On particle Gibbs sampling. *Bernoulli*, 21(3):1855–1883, 2015.
- [6] N. Chopin, S. S. Singh, T. Soto, and M. Vihola. On resampling schemes for particle filters with weakly informative observations. Preprint arXiv:2203.10037, 2022.
- [7] D. Crisan, P. Del Moral, and T. Lyons. Discrete filtering using branching and interacting particle systems. *Markov Process. Related Fields*, 5(3):293–318, 1999.
- [8] P. de Jong and M. J. Mackinnon. Covariances for smoothed estimates in state space models. *Biometrika*, 75(3):601–602, 1988.
- [9] P. Del Moral. Non-linear filtering: interacting particle resolution. *Markov Process. Related Fields*, 2(4):555–581, 1996.
- [10] P. Del Moral. *Feynman-Kac Formulae*. Springer, 2004.

- [11] P. Del Moral. *Mean field simulation for Monte Carlo integration*. Chapman and Hall/CRC, 2013.
- [12] P. Del Moral and L. M. Murray. Sequential Monte Carlo with highly informative observations. *SIAM/ASA Journal on Uncertainty Quantification*, 3(1):969–997, 2015.
- [13] A. Doucet, M. Briers, and S. Sénécal. Efficient block sampling strategies for sequential Monte Carlo methods. *J. Comput. Graph. Statist.*, 15(3):693–711, 2006.
- [14] J. Durbin and S. J. Koopman. *Time series analysis by state space methods*. Oxford University Press, New York, 2nd edition, 2012.
- [15] P. Fearnhead and L. Meligkotsidou. Augmentation schemes for particle MCMC. *Statist. Comput.*, 26(6):1293–1306, 2016.
- [16] Finnish Environment Institute SYKE. CORINE Land Cover 2018. The data are downloaded from the Data Download Service of SYKE on 03.12.2018 under the license CC 4.0 BY, 2018.
- [17] J. M. Flegal and G. L. Jones. Batch means and spectral variance estimators in Markov chain Monte Carlo. *Ann. Statist.*, 38(2):1034–1070, 2010.
- [18] P. W. Glynn and W. Whitt. The asymptotic efficiency of simulation estimators. *Operations research*, 40(3):505–520, 1992.
- [19] P. Guarniero, A. M. Johansen, and A. Lee. The iterated auxiliary particle filter. *J. Amer. Statist. Assoc.*, 112(520):1636–1647, 2017.
- [20] C. A. Hoare. Quicksort. *The Computer Journal*, 5(1):10–16, 1962.
- [21] D. S. Johnson, J. M. London, M.-A. Lea, and J. W. Durban. Continuous-time correlated random walk model for animal telemetry data. *Ecology*, 89(5):1208–1215, 2008.
- [22] S. Karppinen and M. Vihola. Conditional particle filters with diffuse initial distributions. *Statist. Comput.*, 31(3):1–14, 2021.
- [23] A. Lee, S. S. Singh, and M. Vihola. Coupled conditional backward sampling particle filter. Preprint arXiv:1806.05852, 2018.
- [24] F. Lindsten, M. I. Jordan, and T. B. Schön. Particle Gibbs with ancestor sampling. *J. Mach. Learn. Res.*, 15(1):2145–2184, 2014.
- [25] F. Lindsten, P. Bunch, S. S. Singh, and T. B. Schön. Particle ancestor sampling for near-degenerate or intractable state transition models. Preprint arXiv:1505.06356, 2015.
- [26] F. Lindsten, R. Douc, and E. Moulines. Uniform ergodicity of the particle Gibbs sampler. *Scand. J. Stat.*, 42(3):775–797, 2015.
- [27] B. Miasojedow and W. Niemiro. Particle Gibbs algorithms for Markov jump processes. Preprint arXiv:1505.01434, 2015.
- [28] M. Mider, M. Schauer, and F. van der Meulen. Continuous-discrete smoothing of diffusions. Preprint arXiv:1712.03807, 2017.
- [29] S. Särkkä and A. Solin. *Applied stochastic differential equations*, volume 10. Cambridge University Press, 2019.
- [30] S. S. Singh, F. Lindsten, and E. Moulines. Blocking strategies and stability of particle Gibbs samplers. *Biometrika*, 104(4):953–969, 2017.
- [31] M. Vihola, J. Helske, and J. Franks. Importance sampling type estimators based on approximate marginal Markov chain Monte Carlo. Preprint arXiv:1609.02541v3, 2017.
- [32] M. Vihola, J. Helske, and J. Franks. Importance sampling type estimators based on approximate marginal MCMC. *Scand. J. Stat.*, 47(4):1339–1376, 2020.
- [33] N. Whiteley. Discussion on Particle Markov chain Monte Carlo methods. *J. R. Stat. Soc. Ser. B Stat. Methodol.*, 72(3):306–307, 2010.

APPENDIX A. VALIDITY OF CPF WITH KILLING AND SYSTEMATIC RESAMPLING

We start by stating an easy lemma, whose proof is immediate.

Lemma 10. *For a valid conditional resampling scheme $r^{(p,n)}(\cdot \mid g^{(1:N)})$ and its unconditional version r , it holds that:*

- (i) $\mathbb{E}_{r(\cdot \mid g^{(1:N)})} \left[\sum_{i=1}^N \mathbf{1}(A^{(i)} = j) \right] = N \frac{g^{(j)}}{\sum_{i=1}^N g^{(i)}}$ for all $j \in \{1:N\}$, and
- (ii) $r(a^{(1:N)} \mid g^{(1:N)}) \mathbf{1}(a^{(n)} = p) = \frac{g^{(p)}}{\sum_{\ell=1}^N g^{(\ell)}} r^{(p,n)}(a^{(1:N)} \mid g^{(1:N)})$ for all $a^{(i)}$, n and p in $\{1:N\}$.

In what follows, we denote $\underline{M}_1(\underline{x}_1) = \prod_{i=1}^N M_1(x_1^{(i)})$ and $\underline{M}_k(\underline{x}_k \mid x_{k-1}^{(a)}) = \prod_{i=1}^N M_k(x_k^{(i)} \mid x_{k-1}^{(a^{(i)})})$.

Lemma 11. *Suppose that $r^{(p,n)}$ is valid conditional resampling corresponding to unconditional resampling r . If $B_{1:T} \sim U(\{1:N\}^T)$ and $X_{1:T}^* \sim \pi$, then, the particles $\underline{X}_{1:T}$ and the ancestor indices $\underline{A}_{1:T-1}$ generated by Algorithm 3 follow $\pi^{(N)}$.*

Proof. Assume that $X_{1:T}^* \sim \pi$ and $B_{1:T} \sim U(\{1:N\}^T)$ independently. The joint distribution of $B_{1:T}$, the particles $\underline{X}_{1:T}$, and the ancestries $\underline{A}_{1:T-1}$ generated by the CPF, may be written as

$$\begin{aligned}
 & \frac{\underline{M}_1(\underline{x}_1)}{\mathcal{Z} N^T} \left[\prod_{k=2}^T r^{(b_{k-1}, b_k)}(\underline{a}_{k-1} \mid G_{k-1}(\underline{x}_{k-1})) \underline{M}_k(\underline{x}_k \mid x_{k-1}^{(a_{k-1})}) G_{k-1}(\mathbf{x}_{k-1}^{(b_{k-1})}) \right] G_T(\mathbf{x}_T^{(b_T)}) \\
 &= \frac{\underline{M}_1(x_1^{(1:N)})}{\mathcal{Z}} \left(\prod_{k=1}^T \frac{1}{N} \sum_{\ell=1}^N G_k(\mathbf{x}_k^{(\ell)}) \right) \\
 (29) \quad & \left(\prod_{k=2}^T \mathbf{1}(a_{k-1}^{(b_k)} = b_{k-1}) r(\underline{a}_{k-1} \mid G_{k-1}(\underline{x}_{k-1})) \underline{M}_k(\underline{x}_k \mid x_{k-1}^{(a_{k-1})}) \right) \frac{G_T(\mathbf{x}_T^{(b_T)})}{\sum_{\ell=1}^N G_T(\mathbf{x}_T^{(\ell)})},
 \end{aligned}$$

from Lemma 10. Summing over b_1, \dots, b_{T-1} concludes the proof. \square

Proof of Theorem 2. From the proof of Lemma 11, adding the distribution of the variables $\tilde{B}_{1:T}$ to (29) leads to the following extra factor:

$$(30) \quad \left[\prod_{k=2}^T \mathbf{1}(a_{k-1}^{(\tilde{b}_k)} = \tilde{b}_{k-1}) \right] \frac{G_T(\mathbf{x}_T^{(\tilde{b}_T)})}{\sum_{\ell=1}^N G_T(\mathbf{x}_T^{(\ell)})}$$

The joint distribution—product of (29) and (30)—is clearly symmetric with respect to $(b_{1:T}, x_{1:T}^{(b_{1:T})})$ and $(\tilde{b}_{1:T}, x_{1:T}^{(\tilde{b}_{1:T})})$. \square

Proof of Lemma 6 (i). Suppose that $\bar{A}^{(1:N)} \sim \rho(\cdot \mid g^{(1:N)})$, where ρ is given in (6). We first observe that ρ is unbiased:

$$(31) \quad \mathbb{E} \left[\sum_{i=1}^N \mathbf{1}(\bar{A}^{(i)} = j) \right] = \frac{g^{(j)}}{g^*} + \sum_{i=1}^N \left(1 - \frac{g^{(i)}}{g^*} \right) \frac{g^{(j)}}{\sum_{\ell=1}^N g^{(\ell)}} = N \frac{g^{(j)}}{\sum_{\ell=1}^N g^{(\ell)}}.$$

Let $S \in \{1:N\}$ be an independent uniformly distributed random variable, and consider $A^{(1:N)} = \bar{A}^{(\sigma_S(1:N))}$, where

$$\sigma_s(i) := \llbracket i + s \rrbracket_N, \quad \text{with} \quad \llbracket j \rrbracket_N := 1 + (j - 1 \bmod N)$$

is a cyclic permutation of $1:N$. Then $A^{(1:N)} \sim \hat{\rho}(\cdot \mid g^{(1:N)})$, where

$$(32) \quad \hat{\rho}(a^{(1:N)} \mid g^{(1:N)}) := \frac{1}{N} \sum_{s=1}^N \rho(a^{(\sigma_s(1:N))} \mid g^{(1:N)}),$$

which also clearly unbiased, and from (31), it follows that

$$(33) \quad \mathbb{P}(A^{(k)} = j) = \frac{1}{N} \mathbb{E} \left[\sum_{i=1}^N \mathbf{1}(\bar{A}^{(i)} = j) \right] = \frac{g^{(j)}}{\sum_{\ell=1}^N g^{(\ell)}}.$$

Next we derive the conditional distribution of $A^{(-k)}$ given $A^{(k)} = i$. First, because $A^{(k)} = \bar{A}^{(\sigma_S(k))}$, we have

$$\mathbb{P}(\sigma_S(k) = j \mid A^{(k)} = i) = \frac{\mathbb{P}(\sigma_S(k) = j) \mathbb{P}(\bar{A}^{(j)} = i)}{\sum_{\ell=1}^N \mathbb{P}(\sigma_S(k) = \ell) \mathbb{P}(\bar{A}^{(\ell)} = i)} = \frac{\sum_{\ell=1}^N g^{(\ell)}}{N g^{(i)}} \mathbb{P}(\bar{A}^{(j)} = i),$$

and $\mathbb{P}(\bar{A}^{(j)} = i) = \frac{g^{(i)}}{g^*} \mathbf{1}(j = i) + \left(1 - \frac{g^{(i)}}{g^*}\right) \frac{g^{(i)}}{\sum_{\ell=1}^N g^{(\ell)}}$, so a simple calculation yields

$$(34) \quad \mathbb{P}(\sigma_S(k) = j \mid A^{(k)} = i) = h(j \mid i), \quad \text{where } h(j \mid i) := \begin{cases} \frac{1}{N} \left(1 + \frac{\sum_{\ell \neq i} g^{(\ell)}}{g^*}\right), & j = i \\ \frac{1}{N} \left(1 - \frac{g^{(j)}}{g^*}\right), & j \neq i. \end{cases}$$

Note that $\sigma_S(k) = j$ is equivalent with $S = \llbracket j + (N - k) \rrbracket_N$.

We conclude that $A^{(1:N)} \sim \hat{\rho}(\cdot \mid g^{(1:N)})$ may be drawn by first drawing B from the marginal distribution of $A^{(k)}$, that is, $\mathbb{P}(B = i) = g^{(i)} / \sum_{\ell=1}^N g^{(\ell)}$, drawing $J \sim h(\cdot \mid B)$, setting $S = \llbracket J - k \rrbracket_N$ and $\bar{A}^{(\sigma_S(k))} = B$ and $A^{(j)} = \bar{A}^{(\sigma_S(j))}$ for $i \in \{1:N\}$. \square

Lemma 12. *Suppose that ϖ is a permutation of $[N]$, and ϖ_* is a cyclic shift of ϖ , that is, $\varpi_*(i) = \varpi(\sigma_s(i))$ for some $s \in [N]$, and that*

$$\begin{aligned} \bar{A}^{1:N} &= \varpi(F_{\varpi}^{-1}(U^{1:N})) \\ \bar{A}_*^{1:N} &= \varpi_*(F_{\varpi_*}^{-1}(U^{1:N})), \end{aligned}$$

where $U^j = \frac{j-1+U}{N}$ with $U \sim U(0, 1)$.

Then, it holds that $A^{1:N}$ and $A_*^{1:N}$ have the same distribution, where

$$\begin{aligned} A^j &= \bar{A}^{\sigma_C(j)} \\ A_*^j &= \bar{A}_*^{\sigma_C(j)}, \end{aligned}$$

and $C \sim U([N])$ is a random shift offset.

Proof. Without loss of generality, we may consider the case $s = 1$ and $\varpi(i) = i$, in which case $\varpi_*(i) = \sigma_1(i)$.

Define $\tilde{U}^i := (U^i - w^1 \bmod 1)$, let $j = \arg \min_i \tilde{U}^i$, and let $\tilde{U}_*^i = \tilde{U}^{\sigma_j(i)}$. Observe that $\tilde{U}_*^{1:N}$ and $U^{1:N}$ have the same distribution, so the claim follows once we show that $\bar{A}^{1:N} = F^{-1}(U^{1:N})$ and $\bar{A}_*^{1:N} = \sigma_1(F_{\sigma_1}^{-1}(\tilde{U}_*^{1:N}))$ are equal, up to a cyclic shift. Indeed, we will see that for all $i \in [N]$ and $0 \leq k \leq N - 1$:

$$\bar{A}_*^{\sigma_j(i)} = \sigma_1(F_{\sigma_1}^{-1}(\tilde{U}^i)) = k + 1 \iff \bar{A}^i = k + 1.$$

Let us first assume $k \geq 1$, then the expression on the left is equivalent to

$$F_{\sigma_1}(k-1) < \tilde{U}^i \leq F_{\sigma_1}(k) \iff F(k) < \tilde{U}^i + w^1 \leq F(k+1),$$

because $F_{\sigma_1}(\ell) = F(\ell + 1) - w^1$. Whenever $U^i - w^1 \geq 0$, we have $\tilde{U}^i + w^1 = U^i$, and the expression on the right simplifies to $\bar{A}^i = F^{-1}(U^i) = k + 1$, as desired.

Suppose then that $U^i - w^1 < 0$, in which case $\bar{A}^i = F^{-1}(U^i) = 1$. But then also $\tilde{U}^i = U^i - w^1 + 1 \in (1 - w^1, 1)$, which is equivalent to $F_{\sigma_1}^{-1}(\tilde{U}^i) = N$. \square

Proof of Lemma 6 (ii). Assume that ϖ is a permutation (such as the mean partition order). Let $I^{1:N} = F_{\tilde{\varpi}}^{-1}(U^{1:N})$, with

$$U^i = \frac{i - 1 + U}{N},$$

with $U \sim U(0, 1)$, that is, standard systematic resampling (Definition 3) with weights $W_{\tilde{\varpi}}^{1:N}$, where $W_{\tilde{\varpi}}^j = W^{\tilde{\varpi}(j)}$ and $\tilde{\varpi}(j) = \varpi(\sigma_{s-1}(j))$, with $s = \varpi^{-1}(i)$.

Hence, $\tilde{\varpi}$ satisfies

$$(35) \quad \tilde{\varpi}(1) = \varpi(\sigma_{s-1}(1)) = \varpi(s) = i.$$

Define $\bar{A}^{1:N}$ such that

$$\bar{A}^j = \tilde{\varpi}(I^j).$$

Then, by Lemma 12, it holds that

$$A^j = \bar{A}^{\sigma_C(j)}, \text{ for } j \in [N], \text{ with } C \sim U([N]),$$

have the same distribution as the indices from systematic resampling with order ϖ that have been shifted by σ_C . In particular, note that **iii** holds for the latter.

Consider then the count of indices equal to i :

$$N^i = \#\{j : A^j = i\}.$$

Since $A^j = i \iff I^{\sigma_C(j)} = 1$ and the indices $I^{1:N}$ are ascending, it holds that

$$N^i = \max\{j \geq 1 : I^j = 1\},$$

where max is zero in case the set is empty. The event $N^i = n$ is equivalent with

$$\begin{aligned} \frac{n - 1 + U}{N} &< F_{\tilde{\varpi}}(1) \leq \frac{n + U}{N} \\ \iff n - 1 + U &< Nw^i \leq n + U \\ \iff Nw^i - (n - 1) &> U \geq Nw^i - n. \end{aligned}$$

We deduce that only two values of n have nonzero probability (for $U \in (0, 1)$), since:

$$\begin{aligned} n = \lfloor Nw^i \rfloor &\iff U \in [r, 1) \\ n = \lfloor Nw^i \rfloor + 1 &\iff U \in (0, r), \end{aligned}$$

where $r = Nw^i - \lfloor Nw^i \rfloor$. Furthermore, the conditional probabilities for the events $N^i = n$ are given as:

$$\mathbb{P}(N^i = n \mid A^k = i) = \frac{\mathbb{P}(N^i = n, A^k = i)}{\mathbb{P}(A^k = i)} = \frac{\mathbb{P}(N^i = n, A^k = i)}{w^i},$$

where the numerator satisfies

$$\begin{aligned} \mathbb{P}(N^i = n, A^k = i) &= \sum_{c=1}^N \mathbb{P}(C = c, A^k = i \mid N^i = n) \mathbb{P}(N^i = n) \\ &= \sum_{c=1}^N \mathbb{P}(A^k = i \mid C = c, N^i = n) \mathbb{P}(C = c \mid N^i = n) \mathbb{P}(N^i = n). \end{aligned}$$

Since

- $\mathbb{P}(N^i = \lfloor Nw^i \rfloor + 1) = r$ and $\mathbb{P}(N^i = \lfloor Nw^i \rfloor) = 1 - r$ (from above),
- $\mathbb{P}(C = c \mid N^i = n) = 1/N$ (because C is independent of $I^{1:N}$ and therefore N^i),
- $\mathbb{P}(A^k = i \mid C = c, N^i = n)$ are deterministic, either zero or one, and precisely n are one,

it holds that

$$\mathbb{P}(N^i = \lfloor Nw^i \rfloor + 1 \mid A^k = i) = \frac{(\lfloor Nw^i \rfloor + 1)r}{Nw^i} := p,$$

and

$$\mathbb{P}(N^i = \lfloor Nw^i \rfloor \mid A^k = i) = 1 - p.$$

Observe also that the random variable U conditional on $A^k = i$ and $N^i = n$ has the density $U(0, r)$ if $N^i = \lfloor Nw^i \rfloor + 1$ and $U(r, 1)$ if $n = \lfloor Nw^i \rfloor$. This follows since U is conditionally independent from the event $A^k = i$ given $N^i = n$, since U only depends on $A^k = i$ through N^i . Similarly,

$$\mathbb{P}(C = c \mid A^k = i, N^i = n, U) = \mathbb{P}(C = c \mid A^k = i, N^i = n) = \frac{1}{n} \mathbb{1}(\sigma_C(k) \in [1, n]).$$

In practice, we can simulate C from this distribution as follows:

- (1) Draw $\bar{C} \sim U\{1, \dots, n\}$ corresponding to $\sigma_C(k)$ in the above probability,
- (2) set $C = \bar{C} - k$,

since $\sigma_C(k) = \sigma_{\bar{C}-k}(k) \in [1, n]$ is equivalent to $\bar{C} \in [1, n]$. \square

APPENDIX B. VALIDITY OF CPF-BBS

We start by two auxiliary results about marginal distributions after partial ancestor sampling and a partial CPF. In what follows, we assume that $G_k(x_{1:k}) = G_k(x_{k-1:k})$ for $k \in \{2:T\}$. Using the definition of \underline{M}_k as in Appendix A, let us fix some notation: for $u = 1, \dots, T$, denote by $\check{\pi}_u^{(N)}(\underline{x}_{1:u}, \underline{a}_{1:u-1}, b_u)$:

$$\frac{1}{\mathcal{Z}} \underline{M}_1(\underline{x}_1) \prod_{k=1}^{u-1} \left[\left(\frac{1}{N} \sum_{j=1}^N G_k(\mathbf{x}_k^{(j)}) \right) r(\underline{a}_k \mid G_k(\underline{x}_k)) \underline{M}_{k+1}(\underline{x}_{k+1} \mid x_k^{(a_k)}) \right] \frac{G_u(\mathbf{x}_u^{(b_u)})}{N},$$

and $\eta_{u:T}(x_{u:T}) := \prod_{k=u+1}^T M_k(x_k \mid x_{k-1}) G_k(x_{k-1:k})$ with $\eta_{T:T}(x_T) \equiv 1$, then the following define probability distributions for $u = 1, \dots, T$:

$$\mu_u^{(N)}(\underline{x}_{1:u}, \underline{a}_{1:u-1}, b_u, x_{u+1:T}^*) := \check{\pi}_u^{(N)}(\underline{x}_{1:u}, \underline{a}_{1:u-1}, b_u) \eta_{u:T}(x_u^{(b_u)}, x_{u+1:T}^*).$$

Lemma 13. *Suppose that $r^{(p,n)}$ is a valid conditional resampling scheme, with respect to resampling r in Definition 1. Suppose $(\underline{X}_{1:u}, \underline{A}_{1:u-1}, B_u, X_{u+1:T}^*) \sim \mu_u^{(N)}$, and $\ell \in \{1:u-1\}$.*

(i) *If $B_{\ell:u-1} \leftarrow \text{ANCESTORTRACE}(\underline{A}_{\ell:u-1}, B_u)$, then the marginal density of $\underline{X}_{1:\ell}, \underline{A}_{1:\ell-1}, X_{\ell+1:u}^{(B_{\ell+1:u})}, B_{\ell:u}$ and $X_{u+1:T}^*$ is*

$$\mu_\ell^{(N)}(\underline{x}_{1:\ell}, \underline{a}_{1:\ell-1}, b_\ell, x_{\ell+1:u}^{(b_{\ell+1:u})}, x_{u+1:T}^*) / N^{u-\ell}.$$

(ii) *If further $(X_{\ell:u-1}^*, \tilde{B}_{\ell:u-1}) \leftarrow \text{BRIDGECPF}(\mathbf{X}_\ell, B_{\ell:u-1}, X_{\ell:u}^{B_{\ell:u}})$, $\tilde{B}_u = B_u$ and $X_u^* = X_u^{(B_u)}$, then the marginal density of $\underline{X}_{1:\ell}, \underline{A}_{1:\ell-1}, X_{\ell+1:u}^*$ and $\tilde{B}_{\ell:u}$ is*

$$\mu_\ell^{(N)}(\underline{x}_{1:\ell}, \underline{a}_{1:\ell-1}, \tilde{b}_\ell, x_{\ell+1:T}^*) / N^{u-\ell}.$$

Proof. In the case (i), the joint density of all variables may be written as

$$\begin{aligned}
& \check{\pi}_u^{(N)}(\underline{x}_{1:u}, \underline{a}_{1:u-1}, b_u) \left(\prod_{k=\ell}^{u-1} \mathbf{1} \left(b_k = a_k^{(b_{k+1})} \right) \right) \eta_{u:T}(x_u^{(b_u)}, x_{u+1:T}^*) \\
&= \frac{\check{\pi}_\ell^{(N)}(\underline{x}_{1:\ell}, \underline{a}_{1:\ell-1}, b_\ell)}{G_\ell(\mathbf{x}_\ell^{(b_\ell)})} \left[\prod_{k=\ell}^{u-1} \left(\frac{1}{N} \sum_{i=1}^N G_k(\mathbf{x}_k^{(i)}) \right) \mathbf{1} \left(b_k = a_k^{(b_{k+1})} \right) r(\underline{a}_k \mid G_k(\underline{x}_k)) \right. \\
&\quad \left. M_{k+1}(\underline{x}_{k+1} \mid x_k^{(a_k)}) \right] G_u(\mathbf{x}_u^{(b_u)}) \eta_{u:T}(x_u^{(b_u)}, x_{u+1:T}^*) \\
&= \frac{\check{\pi}_\ell^{(N)}(\underline{x}_{1:\ell}, \underline{a}_{1:\ell-1}, b_\ell) \eta_{\ell:T}(x_{\ell:u}^{(b_{\ell:u})}, x_{u+1:T}^*)}{N^{u-\ell}} \prod_{k=\ell}^{u-1} r^{(b_k, b_{k+1})}(\underline{a}_k \mid G_k(\underline{x}_k)) \prod_{i \neq b_{k+1}} M_{k+1}(x_{k+1}^{(i)} \mid x_k^{(a_k)}),
\end{aligned}$$

by Lemma 10 (ii). The result (i) follows as we marginalise $x_u^{(i)}$ for $i \neq b_u$, \underline{a}_{u-1} , $x_{u-1}^{(i)}$ for $i \neq b_{u-1}, \dots, \underline{a}_\ell$.

For (ii), define $\tilde{G}_k^{(\ell,u)}(x_{1:k} \mid x_u) = G_k(x_{k-1:k}) M_{u|\ell}(x_u \mid x_\ell)^{(u-\ell)^{-1}}$, and notice that

$$G_\ell(x_{\ell-1:\ell}) \eta_{\ell:T}(x_{\ell:T}) = \left(\prod_{k=\ell+1}^u \tilde{G}_{k-1}^{(\ell,u)}(x_{1:k-1} \mid x_u) \bar{M}_k(x_k \mid x_{k-1}, x_u) \right) G_u(x_{u-1:u}) \eta_{u:T}(x_{u:T}),$$

where $\bar{M}_u(x_u \mid \cdot, x_u) \equiv 1$. Adding the variables generated in lines 2–7 of Algorithm 8 leads to

$$\begin{aligned}
(36) \quad & \frac{\check{\pi}_\ell^{(N)}(\underline{x}_{1:\ell}, \underline{a}_{1:\ell-1}, b_\ell)}{N^{u-\ell} G_\ell(\mathbf{x}_\ell^{(b_\ell)})} \left[\prod_{k=\ell+1}^{u-1} \tilde{G}_{k-1}(\tilde{\mathbf{x}}_{k-1}^{(b_{k-1})} \mid x_u^{(b_u)}) r^{(b_{k-1}, b_k)}(\tilde{a}_{k-1} \mid \tilde{G}_{k-1}(\tilde{\mathbf{x}}_{k-1} \mid x_u^{(b_u)})) \right. \\
& \quad \left. \left(\prod_{i=1}^N \bar{M}_k(\tilde{x}_k^{(i)} \mid \tilde{x}_{k-1}^{(\tilde{a}_{k-1}^{(i)})}, x_u^{(b_u)}) \right) \right] \tilde{G}_{u-1}(\tilde{\mathbf{x}}_{u-1}^{(b_{u-1})} \mid x_u^{(b_u)}) G_u(x_{u-1:u}^{(b_{u-1:u})}) \eta_{u:T}(x_u^{(b_u)}, x_{u+1:T}^*),
\end{aligned}$$

where $\tilde{\mathbf{x}}_\ell = \underline{\mathbf{x}}_\ell$ and $\tilde{\mathbf{x}}_k^{(i)} = (\tilde{\mathbf{x}}_{k-1}^{(\tilde{a}_{k-1}^{(i)})}, \tilde{x}_k^{(i)})$. Thanks to Lemma 10 (ii)

$$\begin{aligned}
& \tilde{G}_{k-1}(\tilde{\mathbf{x}}_{k-1}^{(b_{k-1})} \mid x_u^{(b_u)}) r^{(b_{k-1}, b_k)}(\tilde{a}_{k-1} \mid \tilde{G}_{k-1}(\tilde{\mathbf{x}}_{k-1} \mid x_u^{(b_u)})) \\
&= \left(\sum_{i=1}^N \tilde{G}_{k-1}(\tilde{\mathbf{x}}_{k-1}^{(i)} \mid x_u^{(b_u)}) \right) \mathbf{1} \left(b_{k-1} = \tilde{a}_{k-1}^{(b_k)} \right) r(\tilde{a}_{k-1} \mid \tilde{G}_{k-1}(\tilde{\mathbf{x}}_{k-1} \mid x_u^{(b_u)})).
\end{aligned}$$

Because the fraction in (36) does not depend on b_ℓ , we may now marginalise over b_ℓ, \dots, b_{u-1} and add the distribution of $\tilde{B}_{u-1} \sim \text{Categ}(\tilde{\omega}_{u-1}^{(1:N)})$ where $\tilde{\omega}_{u-1}^{(j)} = \tilde{G}_{u-1}(\tilde{\mathbf{X}}_{u-1}^{(j)}) G_u(\tilde{X}_{u-1}^{(j)}, X_u^{(B_u)})$, leading into

$$\begin{aligned}
& \frac{\check{\pi}_\ell^{(N)}(\underline{x}_{1:\ell}, \underline{a}_{1:\ell-1}, b_\ell)}{N^{u-\ell} G_\ell(\mathbf{x}_\ell^{(b_\ell)})} \left[\prod_{k=\ell+1}^{u-1} \left(\sum_{i=1}^N \tilde{G}_{k-1}(\tilde{\mathbf{x}}_{k-1}^{(i)} \mid x_u^{(b_u)}) \right) r(\tilde{a}_{k-1} \mid \tilde{G}_{k-1}(\tilde{\mathbf{x}}_{k-1} \mid x_u^{(b_u)})) \right. \\
& \quad \left. \left(\prod_{i=1}^N \bar{M}_k(\tilde{x}_k^{(i)} \mid \tilde{x}_{k-1}^{(\tilde{a}_{k-1}^{(i)})}, x_u^{(b_u)}) \right) \right] \tilde{G}_{u-1}(\tilde{\mathbf{x}}_{u-1}^{(\tilde{b}_{u-1})} \mid x_u^{(b_u)}) G_u(x_{u-1:u}^{(\tilde{b}_{u-1}, b_u)}) \eta_{u:T}(x_u^{(b_u)}, x_{u+1:T}^*).
\end{aligned}$$

Introducing $\tilde{b}_{\ell:u-2}$ by ANCESTORTRACE leads to addition of terms $\mathbf{1}(\tilde{b}_{k-1} = \tilde{a}_{k-1}^{(b_k)})$. Then, calculations similar as above, but in reverse order, lead to (36) with $b_{\ell:u-1}$ replaced with $\tilde{b}_{\ell:u-1}$. The result follows by marginalising over $\tilde{X}_{\ell+1:u-1}$, $\tilde{A}_{\ell+1:u-2}$. \square

Proof of Theorem 8. We start by observing that by Theorem 2, $(\underline{X}_{1:T}, A_{T-1}, \tilde{B}_T) \sim \tilde{\pi}_T^{(N)} = \mu_T^{(N)}$. Then, the proof relies on an iterative application of Lemma 13 (i) and (ii), with $(\ell, u) = (T_{L-1}, T_L), \dots, (T_1, T_2)$, which concludes that $(\underline{X}_1, X_{2:T}^*, \tilde{B}_{1:T}) \sim \mu_1^{(N)}(\underline{x}_1, \tilde{b}_1, x_{2:T}^*)/N^{T-1}$ so $(\tilde{X}_{1:T}^*, \tilde{B}_{1:T}) \sim \mathcal{Z}^{-1}\eta_{1:T}(\tilde{x}_{1:T})/N^T = \pi(\tilde{x}_{1:T})/N^T$. \square

APPENDIX C. COMPUTING THE CONDITIONAL DISTRIBUTIONS IN ASSUMPTION 7 FOR DISCRETISATIONS OF LINEAR SDES

The practical application of Algorithm 7 requires for each block the computation of the conditional distributions $M_{u|\ell}$ and $M_{k|k-1,u}$, where k is a time index in the time discretisation (16), and ℓ and u refer to the block lower and upper boundaries, respectively. This section discusses how these distributions may be computed when:

- $M_{1:T}$ stem from a discretisation of a linear SDE
- $M_{1:T}$ stem from a discretisation of a linear SDE that is conditioned on a set of noisy linear Gaussian observations.

Note that it is enough to only consider the second case, since the first one may be obtained by omitting the conditioning on the observations (see discussion at the end of this section).

Following [29], the conditional means and variance (matrices) of the SDE (15) are given for $t > s$ by

$$(37) \quad \mathbb{E}[X_t \mid X_s = x_s] = \text{expm}(\mathbf{F}(t-s))x_s$$

$$(38) \quad \text{Var}[X_t \mid X_s = x_s] = \int_s^t \text{expm}(\mathbf{F}(t-\tau))\mathbf{K}\mathbf{K}^T\text{expm}(\mathbf{F}(t-\tau))^T d\tau,$$

where expm denotes the matrix exponential. We introduce the notation

$$(39) \quad T_{s,t} := \text{expm}(\mathbf{F}(t-s)), \quad Q_{s,t} := \text{Cov}[X_t \mid X_s = x_s].$$

Assuming a Gaussian initial distribution and the time discretisation (16), we have:

$$(40) \quad \begin{aligned} X_{t_k} \mid X_{t_{k-1}} = x_{t_{k-1}} &\sim N(T_{t_{k-1}, t_k}x_{t_{k-1}}, Q_{t_{k-1}, t_k}) \\ X_{t_1} &\sim N(\mu_{\text{init}}, \Sigma_{\text{init}}), \end{aligned}$$

where μ_{init} and Σ_{init} are the initial mean and variance, respectively.

Suppose then that there are observations $\tilde{Y} = (\tilde{Y}_k)_{k=1, \dots, K_y}$ observed at times \tilde{t}_k , $k = 1, \dots, K_y$, where each observation time is one of the times in time discretisation (16). Further suppose the \tilde{Y}_k are distributed as

$$(41) \quad \tilde{Y}_k \mid X_{\tilde{t}_k} = x_{\tilde{t}_k} \sim N(Z_k x_{\tilde{t}_k}, H_k),$$

where Z_k and H_k are matrices and observation variances, respectively. We may then define the augmented observations $Y = (Y_k)_{k=1, \dots, T}$ with times (16). The random vector Y is distributed like the observations \tilde{Y} at their respective times, and has missing elements otherwise.

Consider then the joint distribution of X_{t_k} , $X_{t_{k-1}}$ and X_{t_u} for $k = \ell + 1, \dots, u - 1$, conditioned on the observations $Y_{1:T} = y_{1:T}$. Since all variables involved are jointly Gaussian, this conditional distribution is:

$$(42) \quad N\left(\begin{bmatrix} \mu_{k|T} \\ \mu_{k-1|T} \\ \mu_{u|T} \end{bmatrix}, \begin{bmatrix} \Sigma_{k|T} & \Sigma_{k,k-1|T} & \Sigma_{k,u|T} \\ \Sigma_{k-1,k|T} & \Sigma_{k-1|T} & \Sigma_{k-1,u|T} \\ \Sigma_{u,k|T} & \Sigma_{u,k-1|T} & \Sigma_{u|T} \end{bmatrix}\right),$$

where we have used the notation

$$\begin{aligned}\mu_{k|n} &:= \mathbb{E}[X_{t_k} \mid Y_{1:n} = y_{1:n}], \\ \Sigma_{k|n} &:= \text{Var}[X_{t_k} \mid Y_{1:n} = y_{1:n}], \\ \Sigma_{p,s|n} &:= \text{Cov}[X_{t_p}, X_{t_s} \mid Y_{1:n} = y_{1:n}].\end{aligned}$$

Here, conditioning on a missing observation should be understood as the observation being removed from the condition.

To obtain the (cross)covariances in (42), the following backwards recursion for $s = t - 1, t - 2, \dots$ from [8] may be used (with a matrix transpose applied to the result as needed):

$$(43) \quad \Sigma_{s,t|T} = \Sigma_{s|s} T_{t_s, t_{s+1}}^T \Sigma_{s+1|s}^{-1} \Sigma_{s+1,t|T}.$$

An inspection of Equations (42) and (43) reveals that all the quantities required are computed routinely by the Kalman filter and smoother [cf. 14] applied to the linear Gaussian state space model composed of (40) and (41). Note that the Kalman filter automatically handles any missing values in the observation sequence.

For $k = \ell + 1$, by elementary properties of the Gaussian distribution, the distribution $M_{u|\ell}$, that is $X_{t_u} \mid X_{t_\ell} = x_{t_\ell}, Y_{1:T} = y_{1:T}$, is

$$(44) \quad \begin{aligned} &N\left(\mu_{u|T} + \Sigma_{\ell,u|T}^T \Sigma_{\ell|T}^{-1} (x_{t_\ell} - \mu_{\ell|T}), \right. \\ &\left. \Sigma_{u|T} - \Sigma_{\ell,u|T}^T \Sigma_{\ell|T}^{-1} \Sigma_{\ell,u|T}\right).$$

Similarly, for $k = \ell + 1, \dots, u - 1$, the distribution $M_{k|k-1,u}$, that is, $X_{t_k} \mid X_{t_{k-1}} = x_{t_{k-1}}, X_{t_u} = x_{t_u}, Y_{1:T} = y_{1:T}$, is

$$(45) \quad \begin{aligned} &N\left(\mu_{k|T} + \Sigma_{k,(k-1,u)|T} \Sigma_{(k-1,u)|T}^{-1} ((x_{t_{k-1}} \ x_{t_u})^T - \mu_{(k-1,u)|T}), \right. \\ &\left. \Sigma_{k|T} - \Sigma_{k,(k-1,u)|T} \Sigma_{(k-1,u)|T}^{-1} \Sigma_{k,(k-1,u)|T}^T\right),\end{aligned}$$

where

$$(46) \quad \begin{aligned}\mu_{(k-1,u)|T} &:= (\mu_{k-1|T} \ \mu_{u|T})^T, \\ \Sigma_{k,(k-1,u)|T} &:= [\Sigma_{k,k-1|T} \ \Sigma_{k,u|T}], \\ \Sigma_{(k-1,u)|T} &:= \begin{bmatrix} \Sigma_{k-1|T} & \Sigma_{k-1,u|T} \\ \Sigma_{u,k-1|T} & \Sigma_{u|T} \end{bmatrix}.\end{aligned}$$

In the case where $M_{1:T}$ simply corresponds to a discretisation of the linear SDE (15), the above computations can be repeated with the conditioned means, variances and covariances replaced with their unconditional counterparts. In practice, an easy way to compute the unconditional means and variances is to set all observations missing in the Kalman filter. The unconditional covariances can then be obtained from (43) as before.

APPENDIX D. MODELS

This section gives additional details related to the models appearing in Section 9.

D.1. CTCRW-P. The CTCRW-P SDE (20) may be placed into the form of the linear SDE (15) by setting

$$X_t = (V_t \ L_t)^T, \ \mathbf{F} = \begin{bmatrix} -\beta_v & 0 \\ 1 & -\beta_x \end{bmatrix} \text{ and } \mathbf{K} = \begin{bmatrix} \sigma & 0 \\ 0 & 0 \end{bmatrix}.$$

The expressions for $T_{s,t}$ and $Q_{s,t}$ in (39) are given as follows. A direct computation yields

$$(47) \quad \expm(Ft) = \begin{bmatrix} \exp(-\beta_v t) & 0 \\ \frac{\exp(-\beta_x t) - \exp(-\beta_v t)}{\beta_v - \beta_x} & \exp(-\beta_x t) \end{bmatrix},$$

when $\beta_v \neq \beta_x$. If $\beta_v = \beta_x$, the first element of the second row is replaced by $t \exp(-\beta_v t)$. The transition matrix $T_{s,t}$ may be obtained from (47) by substituting $t - s$ for t .

If $\beta_v \neq \beta_x$, the elements q_{ij} , $1 \leq i, j \leq 2$ of $Q_{s,t}$ are given by

$$(48) \quad \begin{aligned} q_{11} &= \frac{\sigma^2}{2\beta_v} (1 - \exp(-2\beta_v(t - s))) \\ q_{12} = q_{21} &= \frac{\sigma^2}{\beta_v - \beta_x} \left[\frac{1}{\beta_v + \beta_x} (1 - \exp(-(\beta_v + \beta_x)(t - s))) - \frac{1}{2\beta_v} (1 - \exp(-2\beta_v(t - s))) \right] \\ q_{22} &= \frac{\sigma^2}{(\beta_v - \beta_x)^2} \left[\frac{1}{2\beta_x} (1 - \exp(-2\beta_x(t - s))) + \frac{1}{2\beta_v} (1 - \exp(-2\beta_v(t - s))) \right. \\ &\quad \left. - \frac{2}{\beta_x + \beta_v} (1 - \exp(-(\beta_x + \beta_v)(t - s))) \right]. \end{aligned}$$

If $\beta_v = \beta_x$, the element q_{11} remains as in (48), but the elements q_{12} and q_{22} become:

$$(49) \quad \begin{aligned} q_{12} &= \frac{\sigma^2}{4\beta_v^2} \left[1 + \exp(-2\beta_v(t - s)) \left(-2\beta_v(t - s) - 1 \right) \right], \\ q_{22} &= \frac{\sigma^2}{4\beta_v^3} \left[1 - \exp(-2\beta_v(t - s)) \left(1 + 2\beta_v(t - s)(\beta_v(t - s) + 1) \right) \right]. \end{aligned}$$

Finally, the stationary covariance matrix S with elements s_{ij} used in the initial distribution of the CTCRW-P model is obtained by taking the limit $(t - s) \rightarrow \infty$ in the previous equations:

$$(50) \quad \begin{aligned} s_{11} &= \frac{\sigma^2}{2\beta_v} \\ s_{12} = s_{21} &= \frac{\sigma^2}{\beta_v - \beta_x} \left[\frac{1}{\beta_v + \beta_x} - \frac{1}{2\beta_v} \right] \\ s_{22} &= \frac{\sigma^2}{(\beta_v - \beta_x)^2} \left[\frac{1}{2\beta_x} + \frac{1}{2\beta_v} - \frac{2}{\beta_x + \beta_v} \right], \end{aligned}$$

when $\beta_v \neq \beta_x$. When $\beta_v = \beta_x$, the elements s_{12} and s_{22} are

$$(51) \quad s_{12} = \frac{\sigma^2}{4\beta_v^2} \text{ and } s_{22} = \frac{\sigma^2}{4\beta_v^3}.$$

D.2. CP-RBM. The density of the reflected normal distribution $N^{(r)}(\mu, \sigma^2, a, b)$, for any point x in the support (a, b) , is given by

$$(52) \quad N^{(r)}(x; \mu, \sigma^2, a, b) = N(x; \mu, \sigma^2) + \sum_{k=1}^{\infty} N(g_a^{(k)}(x); \mu, \sigma^2) + N(g_b^{(k)}(x); \mu, \sigma^2),$$

where

$$(53) \quad \begin{aligned} g_a^{(k)}(x) &:= (-1)^k x + ka - kb + (a + b)\mathbf{1} \quad (\text{k odd}) \\ g_b^{(k)}(x) &:= (-1)^k x + kb - ka + (a + b)\mathbf{1} \quad (\text{k odd}). \end{aligned}$$

Equation (52) may be derived by noting that the density of any point $x \in (a, b)$ is equal to the sum of normal densities at points that (eventually) reflect to x . These points consist of x itself and the reflection points outside (a, b) given by the sequences in (53). In practice, we truncate the infinite sum in (52) to the first 10 terms, which provides a reasonable approximation for the values of σ , a and b we use.

D.3. CTCRW. The CTCRW SDE can be placed in the form of the linear SDE (15) by setting

$$X_t = (V_t \ L_t)^T, \quad \mathbf{F} = \begin{bmatrix} -\beta & 0 \\ 1 & 0 \end{bmatrix} \quad \text{and} \quad \mathbf{K} = \begin{bmatrix} \sigma & 0 \\ 0 & 0 \end{bmatrix}.$$

The expressions for $T_{s,t}$ and $Q_{s,t}$ in (39) are then given as follows.

$$(54) \quad T_{s,t} = \begin{bmatrix} \exp(-(t-s)\beta) & 0 \\ \frac{1 - \exp(-(t-s)\beta)}{\beta} & 1 \end{bmatrix},$$

and the matrix $Q_{s,t}$ has elements q_{ij} , $i, j = 1, 2$, such that

$$(55) \quad \begin{aligned} q_{11} &= \frac{\sigma^2}{2\beta} \left(1 - \exp(-(t-s)2\beta) \right), \\ q_{21} = q_{12} &= \frac{\sigma^2}{2\beta^2} \left(1 - 2\exp(-(t-s)\beta) + \exp(-(t-s)2\beta) \right), \\ q_{22} &= \frac{\sigma^2}{\beta^2} \left((t-s) - \frac{2}{\beta} \left(1 - \exp(-(t-s)\beta) \right) + \frac{1}{2\beta} \left(1 - \exp(-(t-s)2\beta) \right) \right). \end{aligned}$$

APPENDIX E. MISCELLANEOUS ALGORITHMS

E.1. Algorithm for finding mean partition order of weights. The following algorithm finds a mean partition order I of the input weights $w^{1:N}$. Note that the algorithm does not modify the weights $w^{1:N}$ and that the operation ‘break’ means exiting from the current (innermost) ‘while’ loop.

E.2. Algorithm for constructing dyadic blocking sequences.

APPENDIX F. DERIVATION OF PLUG

Consider the following artificial conditional particle system that approximates a continuous time conditional particle filter with near constant weights:

- The system has N particles.
- One of the particles corresponds to the ‘reference’, which can not die.
- At most one resampling event occurs at any time k , with probability $p_R^{(k)}$.

Algorithm 12 MEANPARTITIONORDER($w^{1:N}$)

```

1: Set  $p = \text{MEAN}(w^{1:N})$  ('pivot').
2: Set  $i_\ell = 0$  and  $i_u = N + 1$ .
3: Initialise  $I$  as the index set  $[N]$ .
4: while True do
5:   while  $i_\ell < \min(i_u, N)$  do
6:     Set  $i_\ell = i_\ell + 1$ .
7:     Break if  $w^{I^{(i_\ell)}} > p$ .
8:   end while
9:   while  $i_u > i_\ell$  do
10:    Set  $i_u = i_u - 1$ .
11:    Break if  $w^{I^{(i_u)}} < p$ .
12:   end while
13:   Break if  $i_\ell$  equals  $i_u$ .
14:   Swap indices  $i_\ell$  and  $i_u$  of  $I$ .
15: end while
16: output  $I$ 

```

Algorithm 13 DYADICCANDIDATEBLOCKINGS($T \in \{2, 3, \dots\}$)

```

1: Denote by  $p^*$  the largest  $p$  such that  $2^p + 1 \leq T$ .
2: for  $i = 1, \dots, p^* + 1$  do
3:   Set blocksize =  $2^{i-1}$ 
4:   Set  $\ell = 1; u = 0$ .
5:   Set  $k = 0$  (block index)
6:   while  $\ell < T$  do
7:     Set  $k = k + 1$ 
8:     Set  $u = \ell + \text{blocksize}$ 
9:     Set  $T_k^{(i)} = \ell; T_{k+1}^{(i)} = \min(u, T)$ 
10:    Set  $\ell = u$ 
11:   end while
12: end for
13: return Candidate blocking sequences  $T_{1:L^{(i)}}^{(i)}$  for  $i = 1, 2, \dots, p^* + 1$ 

```

- If a resampling event occurs:
 - a dying particle is chosen uniformly among the $N - 1$ particles (excluding the reference).
 - a particle is selected for 'reproduction' uniformly among the $N - 1$ particles (excluding the dying particle).
- If a resampling event does not occur, no particles die or reproduce.

Further suppose that the particle population is divided into two groups, 'ill' and 'healthy', where the ill population is to be interpreted as the particles having reproduced from the reference or any of its descendants. Denote by H_k and $I_k := N - H_k$ the number of healthy and number of ill (including reference) at time k , respectively. Initially, $H_1 = N - 1$.

Theorem 14. *For the artificial particle system of this section, it holds for any $T \geq 1$ that*

$$(56) \quad \mathbb{E}[H_T] = (N - 1) \prod_{k=1}^{T-1} \left(1 - \frac{p_R^{(k)}}{(N - 1)^2} \right).$$

Proof. For any $k \geq 2$ we have

$$H_k \mid H_{k-1} = \begin{cases} H_{k-1} + 1, & \text{prob. } p_{\text{increase}}^{(k-1)} \\ H_{k-1} - 1, & \text{prob. } p_{\text{decrease}}^{(k-1)} \\ H_{k-1}, & \text{prob. } p_{\text{nothing}}^{(k-1)}, \end{cases}$$

where

$$\begin{aligned} p_{\text{increase}}^{(k-1)} &= p_R^{(k-1)} \frac{I_{k-1} - 1}{N - 1} \cdot \frac{H_{k-1}}{N - 1} \quad (\text{resampling occurs, ill dies, healthy reproduces}) \\ p_{\text{decrease}}^{(k-1)} &= p_R^{(k-1)} \frac{H_{k-1}}{N - 1} \cdot \frac{I_{k-1}}{N - 1} \quad (\text{resampling occurs, healthy dies, ill reproduces}), \\ p_{\text{nothing}}^{(k-1)} &= 1 - p_{\text{increase}}^{(k-1)} - p_{\text{decrease}}^{(k-1)}. \end{aligned}$$

Therefore,

$$\begin{aligned} \mathbb{E}[H_T \mid H_{T-1}] &= H_{T-1} + \mathbb{E}[H_T - H_{T-1} \mid H_{T-1}] \\ &= H_{T-1} + p_R^{(T-1)} \frac{I_{T-1} - 1}{N - 1} \cdot \frac{H_{T-1}}{N - 1} - p_R^{(T-1)} \frac{H_{T-1}}{N - 1} \cdot \frac{I_{T-1}}{N - 1} \\ &= \left(1 - \frac{p_R^{(T-1)}}{(N - 1)^2}\right) H_{T-1}, \end{aligned}$$

and

$$\mathbb{E}[H_T] = \mathbb{E}[\mathbb{E}[H_T \mid H_{T-1}]] = \left(1 - \frac{p_R^{(T-1)}}{(N - 1)^2}\right) \mathbb{E}[H_{T-1}],$$

which yields (56) by repeated application. \square

The direct consequence of this result is that $\text{PLUG}(\ell, u)$ equals $\mathbb{E}[H_u/N]$ with $p_R^{(k)} = p_k N$ (defined in Section 7) and ℓ considered as the ‘first’ time point.

APPENDIX G. SUPPLEMENTARY FIGURES

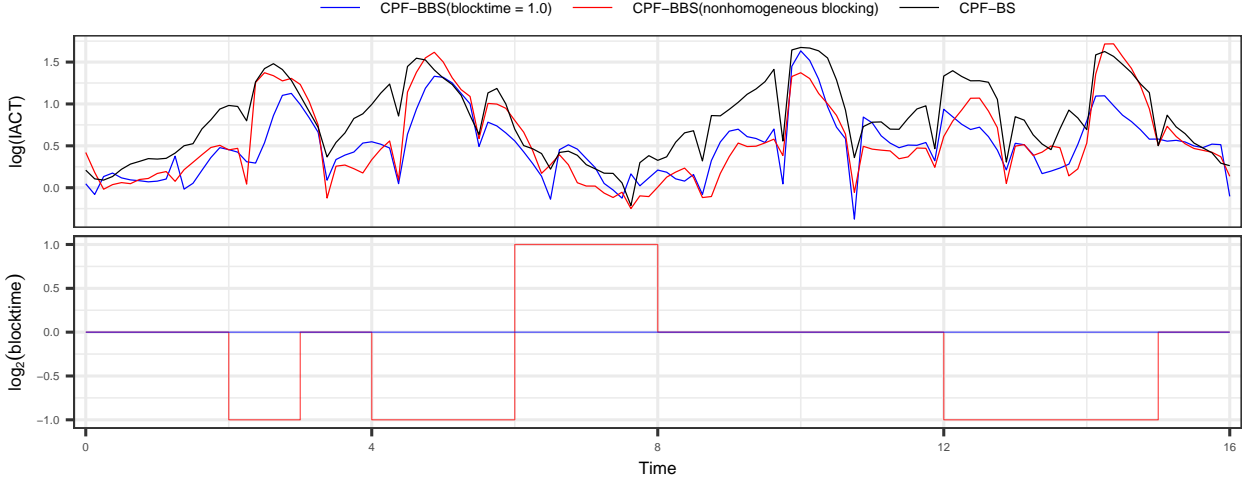


FIGURE 7. Top: The logarithm of the integrated autocorrelation time of the state variable $L_t^{(x)}$ in the CTCRW-T model when the simulation discussed in the text was run with $|\Delta_k| = 0.125$ using the CPF-BS and the CPF-BBS with blocktime 1.0 and the blocking sequence found using Algorithm 11. Bottom: the blocking sequences used in the variants of the CPF-BBS.

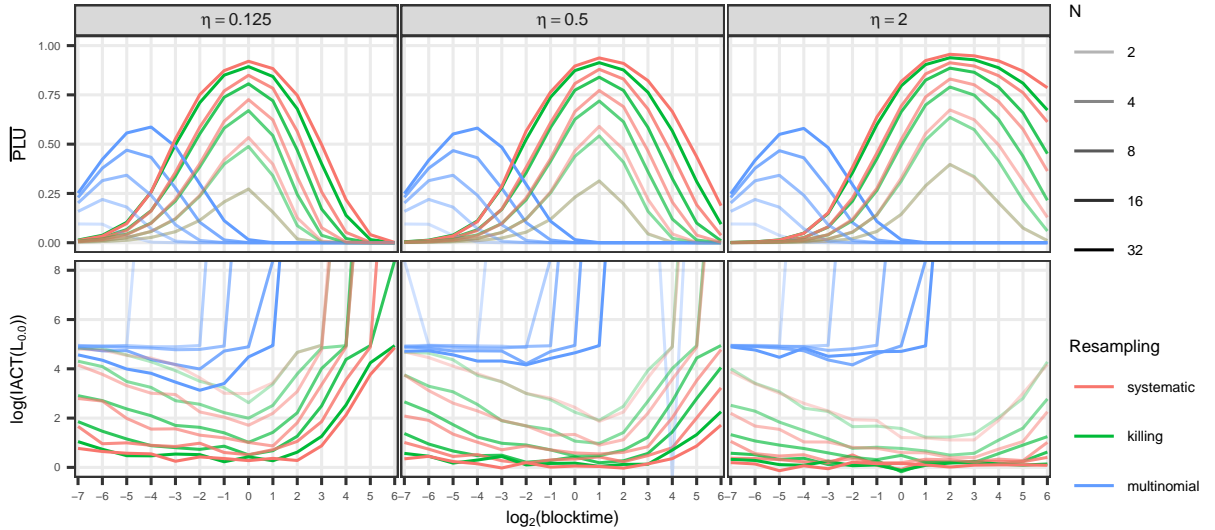


FIGURE 8. The estimated mean probability of lower boundary updates and the logarithm of the integrated autocorrelation time with varying η for the location state variable at time 0.0 in the CTCRW-P model. The colors correspond to conditional systematic, killing and multinomial resamplings, respectively. The transparency of the lines depicts the number of particles used. The horizontal axis gives the value of the blocktime, as described in the text. The value of $|\Delta_k|$ was set to 2^{-7} . The performance of CPF-BS is seen at the far left, with blocktime = 2^{-7} .